



# University of HUDDERSFIELD

## University of Huddersfield Repository

Zhu, Qingyu

Hypercrosslinked Polymer Supported Sulfonic Acids For Esterification of Carboxylic Acids

### Original Citation

Zhu, Qingyu (2013) Hypercrosslinked Polymer Supported Sulfonic Acids For Esterification of Carboxylic Acids. Masters thesis, University of Huddersfield.

This version is available at <http://eprints.hud.ac.uk/id/eprint/19267/>

The University Repository is a digital collection of the research output of the University, available on Open Access. Copyright and Moral Rights for the items on this site are retained by the individual author and/or other copyright owners. Users may access full items free of charge; copies of full text items generally can be reproduced, displayed or performed and given to third parties in any format or medium for personal research or study, educational or not-for-profit purposes without prior permission or charge, provided:

- The authors, title and full bibliographic details is credited in any copy;
- A hyperlink and/or URL is included for the original metadata page; and
- The content is not changed in any way.

For more information, including our policy and submission procedure, please contact the Repository Team at: [E.mailbox@hud.ac.uk](mailto:E.mailbox@hud.ac.uk).

<http://eprints.hud.ac.uk/>

**HYPERCROSSLINKED POLYMER SUPPORTED  
SULFONIC ACIDS FOR ESTERIFICATION OF  
CARBOXYLIC ACIDS**

QINGYU ZHU

A thesis submitted to the University of Huddersfield in  
partial fulfilment of the requirements for the degree of  
Master of Science by Research

University of Huddersfield

June 2013

## Abstract

This work focused on the catalytic performance of hypercrosslinked sulfonic acids for esterification of carboxylic acids. The commercially available hypercrosslinked poly(styrene-divinylbenzene) sulfonic acids, Purolite D5081 and D5082, were found to be more active than macroporous Amberlyst 35 for esterification of long-chained carboxylic acid with methanol. The high activities have been attributed to the high accessibility of the acid sites in the catalysts. However, a relationship between the deactivation of D5081 and D5082 and acid site leaching was observed, and the acid sites were found to leach out only in polar liquids. Further investigation revealed that the leachable acid sites are mainly sulfuric acid trapped in the polymer. Based on these findings, a series of solid sulfonic acids on the hypercrosslinked poly(St-DVB) MN 200 were prepared, with the trapped sulfuric acid thoroughly removed. The surface areas and porosities were measured, and the structures were characterised by solid-state NMR. The home-made catalysts were used for catalysing esterification of acetic acid with methanol, and the catalyst that showed no acid site leaching was used for kinetic modelling for the reaction. It was shown that the Eley-Rideal (single-site) model best fits acetic acid esterification catalysed by the chosen hypercrosslinked sulfonic acid. The home-made catalyst which was highly active and reusable in esterification of pure oleic acid with methanol was tested in esterification of oleic acid esterification blended with rapeseed oil in biodiesel synthesis. The catalytic performance was compared with that of macroporous Amberlyst 35 and gel-type C100X4. The effect of reaction parameters on the reaction kinetics was evaluated for the oil-blended esterification over the hypercrosslinked sulfonic acid catalysis, and the reaction conditions were optimised. Finally, the reusability of the hypercrosslinked sulfonic acid was studied. This home-made hypercrosslinked catalyst in this reaction suffered from deactivation which is due to pore blockage and the loss of functional acid groups. The latter is caused by both sulfonic acid leaching and cation exchange with metal ions in the acidic oil.

## **Acknowledgements**

Foremost, I would like to thank my supervisor Prof. D. R. Brown for his continued support and guidance throughout my research.

A further thank you must be given to Dr. E. A. Dawson who kindly taught me the use of Micromeritics ASAP 2020 analyser.

Special thanks go to Dr. D. C. Apperley who operated the solid-state NMR analysis at the EPSRC National Solid-state NMR Service, Durham University.

I would also like to thank my family and friends for continued encouragement and support throughout this time, especially to the colleagues from the labs of Applied Catalysis.

# Contents

## Glossary

### Chapter 1: Introduction

<b>1.1. Green chemistry</b> .....	9
<b>1.2. Catalysis</b> .....	10
1.2.1. The role of catalysis in green chemistry.....	10
1.2.2. Homogeneous catalysis vs. heterogeneous catalysis.....	11
<b>1.3. Styrene-based sulfonic solid acids</b> .....	13
<b>1.4. Hypercrosslinked polymer: properties and applications</b> .....	14
<b>1.5. Objectives of this project</b> .....	15
<b>1.6. General theories of the characterisation techniques</b> .....	17
1.6.1. Langmuir isotherm and BET isotherm.....	17
1.6.2. The experiment and calculation for surface area.....	19
1.6.3. Pore volume and pore size.....	19
1.6.4. Solid-state NMR.....	20
<b>1.7. A brief review of the kinetics of acid-catalysed esterification reactions</b> .....	21
<b>1.8. A brief review of acid-catalysed esterification of free fatty acids</b> .....	22
<b>References</b> .....	24

### Chapter 2: Catalytic Performance of Purolite D5081 and D5082 in Esterification Reactions and Stability of the Functional Acid Species

<b>2.1. Introduction</b> .....	27
<b>2.2. Experimental</b> .....	27
2.2.1. Materials.....	27
2.2.2. Catalyst characterisation.....	28
2.2.3. Experimental procedure.....	28
<b>2.3. Results and discussion</b> .....	29
2.3.1. Catalyst characterisation.....	29
2.3.2. Catalytic activity.....	30
2.3.3. Reusability of D5081 and D5082.....	33
2.3.4. Acid site leaching of D5081 and D5082 contacted with organic liquids.....	35
2.3.5. Origin of the leachable acid species.....	38
<b>2.4. Summary of results</b> .....	41
<b>References</b> .....	43

## Chapter 3: Preparation, Characterisation and Activity of Home-made Hypercrosslinked Poly(St-DVB) Sulfonic Acids

<b>3.1. Introduction</b>	44
<b>3.2. Experimental</b>	45
3.2.1. Materials	45
3.2.2. Sulfonation procedure	45
3.2.2.1. Route 1	45
3.2.2.2. Route 2	46
3.2.3. Post-treatment of the samples	47
3.2.4. Acid site concentration	47
3.2.5. Surface area and porosity measurement	48
3.2.6. Solid-state NMR	48
3.2.7. Catalytic activity and reusability	49
<b>3.3. Results and discussion</b>	50
3.3.1. Product yield and acid site concentration	50
3.3.2. Surface area and porosity	51
3.3.3. Solid-state NMR	56
3.3.4. Catalytic activity and reusability	57
<b>3.4. Summary of results</b>	62
<b>References</b>	67

## Chapter 4: Kinetics of Acetic Acid Esterification Using Home-made Hypercrosslinked Poly(St-DVB) Sulfonic Acid Catalyst

<b>4.1. Introduction</b>	68
<b>4.2. Experimental and results</b>	68
4.2.1. Elimination of diffusional resistances	68
4.2.2. Kinetic modelling with pseudo-homogenous model	69
4.2.3. Kinetic modelling with the Eley-Rideal model	73
4.2.4. Kinetic modelling with the Langmuir-Hinshelwood model	79
4.2.5. Model verification	81
<b>4.3. Discussion</b>	86
<b>4.4. Summary of results</b>	88
<b>References</b>	89

## Chapter 5: Home-made Hypercrosslinked Poly(St-DVB) Sulfonic Acid Catalysts for the Esterification of Free Fatty Acids in Biodiesel Synthesis

<b>5.1. Introduction</b>	90
<b>5.2. Experimental method and data handling</b>	91
5.2.1. Materials	91
5.2.2. Experimental design	91
5.2.3. Data handling with Analysis of Variance	93

<b>5.3. Results and discussion</b>	96
5.3.1. Catalyst activity in pure oleic acid esterification	96
5.3.2. Catalytic performance in esterification of oleic acid blended with rapeseed oil	98
5.3.2.1. Results of Analysis of Variance	98
5.3.2.2. Effect of catalyst type	99
5.3.2.3. Effect of molar ratio of methanol to FFAs	101
5.3.2.4. Effect of catalyst amount	103
5.3.2.5. Effect of temperature	104
5.3.2.6. Effect of particle size of the catalyst	105
5.3.2.7. Catalyst reusability and deactivation	106
<b>5.4. Summary of the results</b>	108
<b>References</b>	109

## Chapter 6: Conclusion and Suggestions for Future Work

<b>6.1. Conclusion</b>	110
6.1.1. Hypercrosslinked poly(St-DVB) sulfonic acids: activity and reusability	110
6.1.2. Statistical study: kinetic modelling and optimisation of reaction condition	111
<b>6.2. Suggestions for future work</b>	112
6.2.1. More characterisation techniques	112
6.2.2. Improvement of the kinetic model	113
6.2.3. Suitable reactor configuration	114
<b>References</b>	115

## Glossary

This section contains the nomenclature of catalysts mentioned or used in this thesis.

Amberlyst 15: macroporous poly(styrene-divinylbenzene) sulfonic acid.

Amberlyst 16: macroporous poly(styrene-divinylbenzene) sulfonic acid.

Amberlyst 35: 'oversulfonated' macroporous poly(styrene-divinylbenzene) sulfonic acid.

Amberlyst 36: 'oversulfonated' macroporous poly(styrene-divinylbenzene) sulfonic acid.

Amberlyst 131: gel-type poly(styrene-divinylbenzene) sulfonic acid.

Amberlite IR-120: gel-type poly(styrene-divinylbenzene) sulfonic acid.

CT-275: macroporous poly(styrene-divinylbenzene) sulfonic acid.

C100X4: gel-type poly(styrene-divinylbenzene) sulfonic acid.

Dowex 50Wx2: gel-type poly(styrene-divinylbenzene) sulfonic acid.

Purolite D5081: hypercrosslinked poly(styrene-divinylbenzene) sulfonic acid.

Purolite D5082: hypercrosslinked poly(styrene-divinylbenzene) sulfonic acid.

Purolite MN 270: hypercrosslinked poly(styrene-divinylbenzene) sulfonic acid.

Purolite MN 500: hypercrosslinked poly(styrene-divinylbenzene) sulfonic acid.

Purolite MN 200: hypercrosslinked poly(styrene-divinylbenzene) polymer (not functionalised).

Home-made catalysts:

M2A: sulfonic acid functionalised on MN 200 as a part of the work;

M2B: sulfonic acid functionalised on MN 200 as a part of the work;

M2C: sulfonic acid functionalised on MN 200 as a part of the work;

M2D: sulfonic acid functionalised on MN 200 as a part of the work;

M2E: sulfonic acid functionalised on MN 200 as a part of the work.

# Chapter 1

## Introduction

### 1.1. Green chemistry

The term "green chemistry" was coined by Anastas of the US Environmental Protection Agency (EPA) in 1991 [1]. It was soon popularised throughout the world because people are acknowledging the growing need of more sustainable process in the chemical industry. Green Chemistry addresses the development of processes that result in more efficient chemical reactions that preferably utilise renewable raw materials and generate little waste, and reduction or elimination of the use or generation of hazardous substances that have negative impacts on the environment and human health [2]. This concept embodies the 12 principles [1]:

1. Waste prevention instead of remediation,
2. Atom efficiency,
3. Less hazardous/toxic chemicals,
4. Safer products by design,
5. Innocuous solvents and auxiliaries,
6. Energy efficient by design,
7. Preferably renewable raw materials,

8. Shorter synthesis and avoiding derivitisation,
9. Catalytic rather than stoichiometric reagents,
10. Design products for degradation,
11. Analytical methodologies for pollution prevention,
12. Inherently safer processes.

## **1.2. Catalysis**

### 1.2.1. The role of catalysis in green chemistry

Above all the 12 principles, catalysis lies at the heart of waste minimisation and plays a major role in achieving more efficient and economically profitable industrial processes. Today approximately 85-90% of the products of the chemical industry are made in catalytic processes [3]. In some cases, a catalyst is used in place of stoichiometric reagents in order to efficiently use the raw materials and to reduce waste [3]. In general, a catalyst is used to lower the activation energy of the reaction, affording alternative reaction pathway (**Fig. 1.1**). The successful choice of catalyst for a reaction lies in lowering the required energy input, acceleration of rate of reaction, and high selectivity to the desired product.

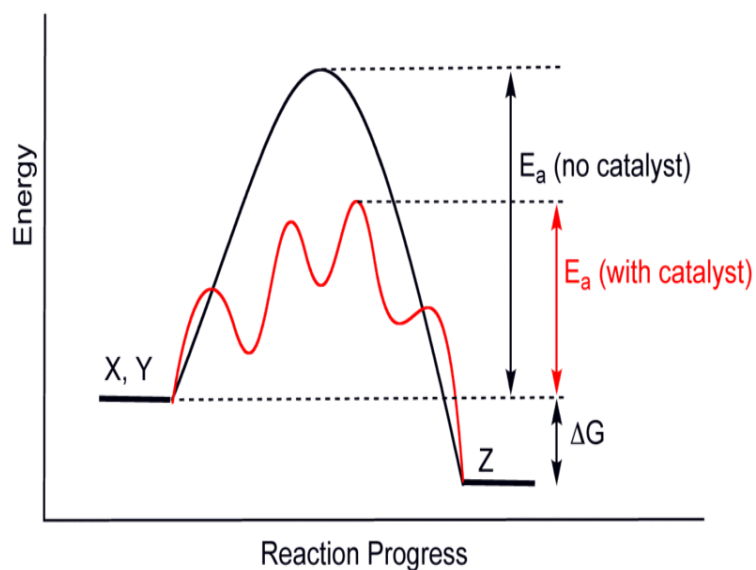


**Fig. 1.1.** The energy profiles of reaction progress in the catalytic reaction and the non-catalytic reaction.

### 1.2.2. Homogeneous catalysis vs. heterogeneous catalysis

Catalysis is commonly divided into two main categories, homogeneous catalysis and heterogeneous catalysis. Homogeneous catalysis means catalysts are in the same phase as the reactants and are equally dispersed in the reaction medium. Heterogeneous catalysis takes place between different phases, the catalyst is generally a solid and the reactants are gases or liquids. The comparison of homogeneous catalysis and heterogeneous catalysis is summarised in **Table 1.1**.

Homogeneous catalysts are in use in many chemical processes due to their high activity and selectivity. They are sometimes strong mineral acids or Lewis acids which are toxic and corrosive. The environmentally associated problems of handling, removal and disposal of corrosive waste are encouraging the application of their heterogeneous alternatives.

**Table 1.1.** Comparison of homogeneous and heterogeneous catalysis [4]

<b>Homogeneous catalysis</b>	<b>Heterogeneous catalysis</b>
<b>Often difficult to separate</b>	Readily separated
<b>Expensive to recycle</b>	Readily regenerated and recycled
<b>not diffusion controlled</b>	May be diffusion limited
<b>Usually robust to poisons</b>	Sensitive to poisons
<b>Higher selectivity</b>	Lower selectivity
<b>Short service life</b>	Long service life
<b>Often take place under mild conditions</b>	Often higher energy process

Acid-catalysed processes constitute one of the most important applications of heterogeneous catalysis. A wide variety of solid acids are used in the chemical industry, such as acidic clays, mixed metal oxides, zeolites and zeotypes, supported heteropoly acids, and sulfonic acid supported by mesoporous silicas or polymers. [1]. Reactions over heterogeneous catalyst involve diffusion, adsorption and desorption processes apart from the actual chemical reaction. In the reaction on a porous solid the following steps are expected [5]:

1. Diffusion of the reactants through the boundary layer to the catalyst surface;
2. Diffusion of the reactants into the pores;
3. Adsorption of the reactants on the surface of the pores;
4. Chemical reaction on the catalyst surface;
5. Desorption of the products out of the pores;
6. Diffusion of the products away from the catalyst through the boundary layer and into the reaction mixture.

The measured reaction rate is determined by the rate of slowest step which is normally the surface reaction on the catalyst. The mathematical expression of the catalytic process often includes a combination of energetics of adsorption and the chemical reaction.

### **1.3. Styrene-based sulfonic acids**

This category of solid acids is of a sulfonic acid moiety attached to the surface, which are heterogeneous equivalents to the homogeneous catalysts,  $H_2SO_4$ . Prior to 1960, styrene-based polymer resins were gel-type, which were copolymers of styrene (St) with a small portion (typically 5-8%) of divinylbenzene (DVB) at a low monomer dilution [6, 7]. The gel-type resins have no permanent porosity. The pores are only formed in the swollen state and are micropores or small mesopores, depending on the swelling and degree of crosslinking [8]. In non-swelling media, the active sites in the interior of the functionalised resin are largely inaccessible.

The problem of active site accessibility was overcome with the development of macroporous styrene-based resins. The macroporous resin consists of styrene cross-linked with 12-20% of divinylbenzene, leading to a high inner surface area typically ca.  $40\text{ m}^2/\text{g}$  [7]. The permanent porosity is achieved by incorporating an inert porogen compound at the polymerisation stage. As a result, these macroporous resins can function in non-swelling solvents, which greatly expands the possibility of application of these materials as catalysts. A range of catalysed

esterifications, as well as other reactions, has spearheaded the industrial importance of these resins supporting sulfonic acids [9-12].

#### **1.4. Hypercrosslinked polymer: properties and applications**

The third generation of styrene-based resins is the hypercrosslinked styrene-based polymer which was initially introduced by Davankov and colleagues in the 1970s [13]. The hypercrosslinked poly(St-DVB) resins, for example, are prepared by extensive post-crosslinking of highly solvated gels of poly(St-DVB) beads with numerous rigid bridging methylene groups in the presence of Friedel-Crafts catalysts [14, 15]. The cross-linking bridges are homogeneously distributed throughout the whole volume of the polymer, which leads to a uniform single-phase network [16]. The inner stresses of the hypercrosslinked resin are preferably relaxed in the swollen state. For this reason, combined with restricted configurational flexibility by rigid bridges, the hypercrosslinked resins tend to expand even in weak interaction with non-solvent [16, 17]. The expansion of the polymer network and the relaxation of inner strains facilitate its promising behaviour in sorption. In fact, hypercrosslinked polymers have been extensively applied for hydrogen storage [18], packing materials for HPLC [19], organic vapour sorption [20], and removal of organic compounds and toxic metals from waste water [21, 22]. The sorption capacity of hypercrosslinked resins was reported as being up to three times higher than macroporous resins [22].

The average size of the pores in the hypercrosslinked polystyrene was found to be 1.5-3.0 nm [14]. The large number of nanopores can serve as nanoreactors which control the migration and growth of nanocomposites. For example, palladium nanoparticles were obtained by impregnating  $\text{Na}_2\text{PdCl}_4$  to hypercrosslinked MN 270 in mixture of  $\text{H}_2\text{O}$  and MeOH dissolved in THF [23]. This metal/polymer nanocomposite exhibited high activity and in selective hydrogenation of acetylene alcohols.

The hypercrosslinked polymer is also able to be functionalised, and the sorption capacity can be remarkably increased after functionalising with  $-\text{SO}_3\text{H}$  groups [24]. Inspired by the application of the sulfonated macroporous styrene-based resins as catalysts, it was thought that the sulfonated hypercrosslinked resins would be able to act as solid acid catalysts in some reactions due to their high surface area and porosity. Therefore, the target of this project was to evaluate the catalytic performance of hypercrosslinked polymer supported sulfonic acids in organic reactions. The sulfonic acid was to be functionalised on the hypercrosslinked poly(St-DVB) and esterification of carboxylic acids with methanol was chosen as the model reaction.

### **1.5. Objectives of this project**

This project focuses on the catalytic performance of hypercrosslinked poly(St-DVB) supported sulfonic acids in esterification of carboxylic acids. The specific objectives are the following:

- i. To evaluate the activity of hypercrosslinked poly(St-DVB) sulfonic acids Purolite D5081 and D5082 in esterification of different carboxylic acids;
- ii. To understand the leaching of acid sites in Purolite D5081 and D5082 in contact with organic compounds and water, and the origin of the leachable acid species;
- iii. To understand the use of characterisation techniques in characterising the surface area and porosity of solid acids;
- iv. To find relationships among sulfonation, structural characteristics and catalytic performance of hypercrosslinked poly(St-DVB) sulfonic acids in the esterification of carboxylic acids;
- v. To understand the mechanistic pathway of the esterification reaction catalysed by hypercrosslinked poly(St-DVB) sulfonic acid;
- vi. To compare the activities of hypercrosslinked, macroporous, gel-type resin supported sulfonic acids in esterification of free fatty acids, and the effect of reaction parameters on activity of the hypercrosslinked poly(St-DVB) sulfonic acid in this reaction;
- vii. To study the activity and reusability of the hypercrosslinked poly(St-DVB) sulfonic acid in esterification of free fatty acids in biodiesel synthesis.

## 1.6. General theories of the characterisation techniques

### 1.6.1. Langmuir isotherm and BET isotherm

The Langmuir is based on the chemisorption model in which adsorption is limited to monolayer on the solid. The following assumptions are made [25]:

1. Adsorption occurs on specific sites;
2. All adsorption sites are identical;
3. The energy for adsorption is independent of how many neighbouring sites are occupied.

The Langmuir equation isotherm corresponds to equilibrium in which the rates of adsorption and desorption are equal. In the case of a single adsorbing gas onto the surface, the Langmuir equation is:

$$\frac{P}{V} = \frac{1}{V_m} P + \frac{1}{kV_m}, \quad (\text{Eq. 1.1})$$

where  $P$  is the equilibrium pressure over the solid,  $V$  is the actual volume adsorbed,  $V_m$  is volume of the gas required to produce monolayer coverage, and  $k$  is the Langmuir factor in which the activation energy and collision rate are taken into account:

$$k = \frac{A \exp\left(\frac{-E_a + E_d}{RT}\right)}{N_s \sqrt{2\pi m k_B T}}, \quad (\text{Eq. 1.2})$$

where A is the exponential factor,  $E_a$  and  $E_d$  are the activation energies of adsorption and desorption of an adsorbate on the surface respectively, R is the ideal gas constant, T is temperature,  $N_s$  is the number of sites available for adsorption,  $\pi$  is the ratio of a circle's circumference to its diameter, m is the molecular mass of the adsorbate and  $k_B$  is Boltzmann's constant. The Langmuir model was extended by Brunauer, Emmett and Teller to encompass multilayer adsorption. Additional assumptions are made [25]:

1. Each layer of adsorbate is treated as a Langmuir monolayer and must be completed before the next layer starts to form;
2. The heat of adsorption for the first layer is characteristic of the adsorbate;
3. The heat of adsorption for subsequent layers is equal to the heat of condensation.

If volumetric measurements are taken the BET equation is generally given as:

$$\frac{P}{V(P_0 - P)} = \frac{C - 1}{V_m C} \times \frac{P}{P_0} + \frac{1}{V_m C} \quad (\text{Eq. 1.3})$$

where P and  $P_0$  are the equilibrium and the saturation pressure of adsorbates at the temperature of adsorption, V and  $V_m$  are the adsorbed gas quantity and the monolayer adsorbed gas quantity and C is the BET constant.

### 1.6.2. The experiment and calculation for surface area

The surface area of a porous solid is normally calculated from a plot of the linearised form of the Langmuir or BET equations, by measuring the quantity of gas adsorbed on the surface over a range of gas pressure. Experimentally, the solid sample is pre-treated to remove adsorbed contaminants, and is then cooled under vacuum. An adsorbate is dosed to the solid in controlled increments. After each dose of adsorbate, the pressure is allowed to equilibrate. The volume adsorbed ( $V$ ) at each pressure and constant temperature defines an adsorption isotherm. The volume of gas required to form a complete monolayer over the surface of the solid ( $V_m$ ) is determined by the uptake of the adsorbed gas. Therefore, the specific surface area of the porous solid can be calculated from

$$\text{Surface area} = \frac{NA_{cs}}{vm} \times V_m, \quad (\text{Eq. 1.4})$$

where  $N$  is Avogadro's number,  $A_{cs}$  is the cross-sectional area of the adsorbing species,  $v$  is the molar volume of the adsorbate gas, and  $m$  is the mass of the adsorbent. Typically nitrogen is used as adsorbate and its effective cross-sectional area is taken as  $0.1620 \text{ nm}^2$  provided it is not affected by the nature of the solid.

### 1.6.3. Pore volume and pore size

The phenomenon of capillary condensation provides a method for analysing the fine pore structures. As the pressure is increased, the gas condenses firstly in pores of smallest dimensions and progresses to larger pores until saturation is reached. The

pore volume ( $V_p$ ) can be calculated from the amount of gas adsorbed at appropriate pressures. Pore size distribution is illustrated from experimental isotherms by the Barrett, Joyner and Halenda (BJH) method [26], which is essentially a modification of Kelvin equation:

$$\ln\left(\frac{P}{P_0}\right) = -\frac{2\sigma V_p}{r_p RT}, \quad (\text{Eq. 1.5})$$

where  $P$  is the actual vapour pressure,  $P_0$  is the saturated vapour pressure,  $\sigma$  is the surface tension,  $V_p$  is the pore volume,  $r_p$  is the pore radius,  $R$  is the ideal gas constant and  $T$  is temperature.

The radius of the pore is calculated from the radius given by the Kelvin equation, corrected for the thickness of a liquid film which adheres to the pore walls. Using the assumption that the pores are of cylindrical geometry, the pore radius ( $r_p$ ) is calculated from the ratio of BET surface area ( $A_{\text{BET}}$ ) and pore volume ( $V_p$ ):

$$r_p = \frac{2V_p}{A_{\text{BET}}}. \quad (\text{Eq. 1.6})$$

#### 1.6.4. Solid-state NMR

Solid-state NMR can be used to determine the molecular information which is characterised by the presence of anisotropic interactions [27]. High resolution conditions in solids can be established using magic-angle spinning which enables to remove the effects of chemical shift anisotropy in solids by seating the axis of rotation at an angle of  $54.74^\circ$ , and to zero the secular terms of dipolar coupling with rapid spinning rate [28]. Cross-polarisation technique (CP) can be used to assist

signal enhancement of dilute spins. For the study of sulfonated polystyrene resins, solid-state  $^{13}\text{C}$  and  $^1\text{H}$  NMR are potentially useful. It would be expected that  $^{13}\text{C}$  chemical shifts associated with benzene rings and with bridging methylene groups might be sensitive to functionalisation with sulfonic acids. On this basis,  $^1\text{H}$  spectra might also show some dependence.

### **1.7. A brief review of kinetics of acid-catalysed esterification reactions**

Strong mineral acids, such as  $\text{H}_2\text{SO}_4$  and  $\text{HCl}$ , have been extensively studied for catalysing esterification of carboxylic acids with alcohols [29]. It is known that the mechanism firstly involves protonation of the carboxylic acid, which was attacked by nonprotonated alcohol. The product ester is obtained following the proton transfer and dehydration of the protonated carboxylic acid. The rate limiting step of the esterification is the nucleophilic attack of the alcohol on the protonated carbonyl group of the carboxylic acid [30].

As heterogeneous alternatives to the mineral acids for esterification reactions, solid catalysts with Bronsted acid sites are expected similar behaviour with a homogeneous-like mechanism. However, the mechanism of solid-acid catalysed esterification was ambiguously reported in the literature. A simple pseudo-first order kinetics of the carboxylic acid was found to fit the esterification of lactic acid with isopropanol over acid ion-exchange resins (Amberlyst 15 and Amberlyst 36) [31]. Models which take account of the reverse as well as the forward reaction as the reaction approaches equilibrium have been used to fit the observed kinetics of

esterification of acetic acid with isobutanol catalysed by Dowex 50 Wx2 and Amberlyte IR-120 [32], and the esterification of fatty acids by Purolite CT-275 [33]. Moreover, Tesser et al have successfully applied the Eley-Rideal (single-site) model to interpret the kinetics of oleic acid esterification with methanol in the presence of triglycerides with Relite CFS [34] and Amberlyst 15, 16 and 131 [35]. The application this model was also reported by Liu et al to fit the esterification of acetic acid with methanol over silica supported sulfonic acids [36]. On the contrary, Miao et al argued that the Langmuir-Hinshelwood (dual-site) model better fits the behaviour of acetic acid esterification with methanol on mesoporous silica solid acid [37]. In the case of acetic acid esterification with n-butanol on Amberlyst 15, Gangadvala et al applied a modified Langmuir-Hinshelwood model by involving the effect of water distribution in the resin phase [38]. Additionally, Tsai et al found that the Eley-Rideal and the Langmuir-Hinshelwood models equally well fit the experimental data for the acetic acid esterification over Amberlyst 36 [39].

### **1.8. A brief review of acid-catalysed esterification of free fatty acids**

To remove the high free fatty acid (FFA) content in oil feedstock for biodiesel production, some researchers have proposed a two-step process that the acidic oil first undergoes acid-catalysed esterification before transesterification of the triglycerides. Sulfuric acid and heteropoly acids are effective to remove the FFAs [29, 40]. However, the use of homogeneous catalysts is associated with effluent disposal problems and equipment corrosion [41]. These drawbacks have led to research into

the application of solid acid catalysts. To date, modified zeolite, functional activated carbons, supported heteropoly acids, resin-typed nafion, sulfonic acid on mesoporous silicas and zirconium cation clusters have been reported as active acid catalysts for the esterification for biodiesel synthesis [42-48]. Alternatively a range of macroporous poly(St-DVB) supported sulfonic acids have also been intensively studied for the esterification of FFAs [49-51].

## References

- [1] R. A. Sheldon, I. Arends and U. Hanefeld, *Green Chemistry and Catalysis*, Wiley-VCH, Weinham, 2007.
- [2] M. Doble and A. K. Kruthiventi, *Green Chemistry and Engineering*, Elsevier, Burlington, 2007.
- [3] I Chorkendorff and J. W. Niemantsverdriet, *Concepts of Modern Catalysis and Kinetics* (2<sup>nd</sup> ed.), Wiley-VCH, Weinheim, 2007.
- [4] M. Lancaster, *Green Chemistry: an Introductory Text* (2<sup>nd</sup> ed.), RSC, Cambridge, 2010.
- [5] J. Hagen, *Industrial Catalysis: A Practical Approach* (2<sup>nd</sup> ed.), Wiley-VCH, Weinheim, 2006.
- [6] A. M. S. Oancea, C. Drinkal and W. H. Holl, *React. & Funct. Polym.*, 68 (2008) 492-506.
- [7] B. M. E. Russbueltdt and W. F. Hoelderich, *Appl. Catal. A: Gen.*, 362 (2009) 47-57.
- [8] F. M. B. Coutinho, R. R. Souza and A. S. Gomes, *Europ. Polym. J.*, 40 (2004) 1525-1532.
- [9] C. Pirola, C. L. Bianchi, D. C. Boffito, G. Carvoli and V. Ragaini, *Ind. Eng. Chem. Res.*, 49 (2010) 4601-4606.
- [10] M. Petrini, R. Ballini, E. Marcantoni and G. Rosini, *Synth. Commun.*, 18 (1988) 847-853.
- [11] V. K. S. Pappu, A. J. Yanez, L. Peereboom, E. Muller, C. T. Lira and D. J. Miller, *Bioresour. Technol.*, 102 (2011) 4270-4272.
- [12] S. Kimura, K. Manabe and S. Kobayashi, *Org. Biomol. Chem.*, 1 (2003) 2416-2418.
- [13] V. A. Davankov, M. P. Tsyurupa, and S. V. Rogozhin, *J. Polym. Sci. Symp.*, 47 (1974) 95-101.
- [14] M. P. Tsyurupa and V. A. Davankov, *React. & Funct. Polym.*, 66 (2006) 768-779.
- [15] M. P. Tsyurupa, Z. K. Blinnikova, N. A. Trosturina, A. V. Pastukhov, L. A. Pavlova and V. A. Davankov, *Nanotechnol. Russian*, 4 (2009) 665-675.
- [16] M. P. Tsyurupa and V. A. Davankov, *React. & Funct. Polym.*, 53 (2002) 193-203.
- [17] X. Zhang, S. Shen and L. Fan, *J. Mater. Sci.*, 42 (2007) 7621-7629.
- [18] J. Germain, F. Svec and J. M. J. Frechet, *Chem. Mater.*, 20 (2008) 7069-7076.
- [19] V. A. Davankov, M. P. Tsyurupa and N. N. Alexienko, *J. Chromatogr. A*, 1100 (2005) 32-39.

- [20] V. V. Podlesnyuk, J. Hradil and E. Kralova, *React & Funct. Polym.*, 42 (1999) 181-191.
- [21] P. Veverka and K. Jerabek, *React & Funct. Polym.*, 59 (2004) 71-79.
- [22] V. V. Azanova and J. Hradil, *React. & Funct. Polym.*, 41 (1999) 163-175.
- [23] E. M. Sulman, L. Zh. Nikoshvili, V. G. Natveeva, I. Y. Tyamina. A. I. Sidorov, A. V. Bykov, G. N. Demidenko, B. D. Stein and L. M. Bronstein, *Top Catal.* 55 (2012) 492-497.
- [24] B. Li, F. Su, H. Luo, L. Liang and B. Tan, *Micro. & Meso. Mater.*, 138 (2011) 207-214.
- [25] E. M. McCash, *Surface Chemistry*, Oxford University Press, New York, 2001.
- [26] E. P. Barrett, L. G. Joyner and P. P. Halenda, *J. Am. Chem. Soc.*, 73 (1951) 373-380
- [27] M. J. Duer, *Introduction to Solid-state NMR Spectroscopy*, Blackwell Publishing, Oxford, 2004.
- [28] T. C. Pochapsky and S. S. Pochapsky, *NMR for Physical and Biological Scientists*, Garland Science, New York, 2007.
- [29] J. M. Marchetti and A. F. Errazu, *Biomass. & Bioen.*, 32 (2008) 892-895
- [30] E. Lotero, Y. J. Liu, D. E. Lopez, K. Suwannakarn, D. A. Bruce and J. G. Goodwin Jr., *Ind. Eng. Chem. Res.*, 44 (2005) 5353-5363.
- [31] G. D. Yadav and H. B. Kulkarni, *React. & Funct. Polym.*, 44 (2000) 153-165.
- [32] A. Izci and F. Bodur, *React. & Funct. Polym.*, 67 (2007) 1458-1464.
- [33] S. Pasiyas, N. Barakos, C. Alexopoulos and N. Papayannakos, *Chem. Eng. Technol.*, 29 (2006) 1365-1371.
- [34] R. Tesser, M. Di Serio, M. Guida, M. Nastasi and E. Santacesaria, *Ind. Eng. Chem. Res.*, 44 (2005) 7978-7982.
- [35] R. Tesser, L. Casale, D. Verde, M. Di Serio and E. Santacesaria, *Chem. Eng. J.*, 157 (2010) 539-550.
- [36] Y. Liu, E. Lotero and J. G. Goodwin Jr, *J. Catal.*, 242 (2006) 278-286.
- [37] S. Miao and B. H. Shanks, *J. Catal.*, 279 (2011) 136-143.
- [38] J. Gangadwala, S. Mankar, S. Mahajani, A. Kienle and E. Stein, *Ind. Eng. Chem. Res.*, 42 (2003) 2146-2155.
- [39] Y. Tsai, H. Lin and M. Lee, *Chem. Eng. J.*, 171 (2011) 1367-1372.
- [40] A. L. Cardoso, R. Augusti and M. J. Da Silva, *J. Am. Oil Chem. Soc.*, 85 (2008) 555-560.

- [41] K. Wilson and J. H. Clark, *Pure Appl. Chem.*, 72 (2000) 1313-1319.
- [42] K-H. Chung, D-R. Chang and B-G. Park, *Biores. Technol.*, 99 (2008) 7438-7443.
- [43] A. Ahdana-Perez, L. Lartumdo-Rojas, T. Gomez, M. E. Nino-Gomez, *Fuel*, 100 (2012) 128-138.
- [44] A. Alsalme, E. F. Kozhevnikova and I. V. Kozhevnikov, *Appl. Catal., A: Gen.*, 349 (2008) 170-176.
- [45] M. Alvaro, A. Corma, D. Das, V. Fornes and H. Garcia, *J. Catal.*, 231 (2005) 48-55.
- [46] I. S. Mbaraka, D. R. Radu, V. S. Lin and B. H. Shank, *J. Catal.*, 219 (2003) 329-336.
- [47] K. Manti, K. Komura and Y. Sugi, *Green Chem.*, 7 (2005) 677-682.
- [48] F. Omata, A. C. Dimian and A. Bliiek, *Chem. Eng. Sci.*, 58 (2003) 3175-3185.
- [49] A. Ramadhas, S. Jayaraj and C. Mraleedharan, *Fuel*, 98 (2005) 335-340.
- [50] J. Y. Park, D. K. Kim and J. S. Lee, *Bioresour. Technol.* 101 (2010) 62-65.
- [51] S. Gan, H. K. Ng, P. H. Chan and F. L. Leong, *Fuel Process Technol.*, 102 (2012) 67-72.

## Chapter 2

# Activity of Purolite D5081 and D5082 in Esterification Reactions and Stability of the Functional Acid Species

### 2.1. Introduction

Esterification is the transformation of carboxylic acids or their derivatives into esters, and it is greatly important in the production of flavours, pharmaceuticals, plasticisers and polymerisation monomers, as well as for protection of carboxylic acids and hydroxyl groups in organic synthesis [1, 2]. The esterification reactions are usually conducted in liquid or vapour phase with the aid of acid or base catalysts.

To gain insight into the catalytic performance of hypercrosslinked polymer supported sulfonic acids in the esterification reactions, Purolite D5081 and D5082 which are sulfonated hypercrosslinked poly(St-DVB) were evaluated as the catalysts. Reusability and deactivation of these catalysts were also investigated. The focus was on the stability of the functional acid species during the reaction and in contact with organic liquids and water.

### 2.2. Experimental

#### 2.2.1. Materials

Acetic acid (99.7+ %), oleic acid (99.7+ %) and methanol (99.5+ %) were purchased from Fisher Scientific, UK. The sulfonated hypercrosslinked poly(St-DVB) resins, D5081 and D5082 were provided by Purolite Int. Ltd. UK. The macroporous

poly(St-DVB) resin Amberlyst 35 (wet) was from Rohm & Haas France S.A.S. The resins were washed with acetone, and were dried in the oven at 80 °C overnight.

### 2.2.2. Catalyst characterisation

Acid site concentrations of the catalysts were determined by acid-base back titration. A weighed amount of the dry catalyst was put in contact with 0.100 M NaOH solution in excess for two hours. The excess base was titrated with 0.100 M HCl solution and phenolphthalein as the indicator. Several repetitions were made in order to control the error within 0.05 mmol/g of dried catalysts. In the measurement of remaining acid sites of D5081 in water, the errors were controlled within 0.02 mmol/g.

Surface area and porosity measurements were carried out by nitrogen adsorption-desorption method using the Micromeritics ASAP 2020 analyser. Surface areas were calculated by the BET method. Pore volumes and pore sizes were calculated from desorption isotherms using the BJH method.

### 2.2.3. Kinetic measurements

The experiments were conducted in a batch reactor equipped with magnetic stirrer and water-cooled condenser. A thermocouple was placed in the reactor to control the temperature within  $\pm 1$  °C. 4.00 g carboxylic acid and 20.0 g methanol were charged into the reactor, and the mixture was stirred at 600 rpm to eliminate possible external mass transfer limitation. When the mixture reached a temperature of 65 °C, 0.200 g of catalyst was charged to the reactor. This was considered as the starting time of the reaction. Samples of the mixture were withdrawn at regular

intervals to monitor the conversion of carboxylic acid which was quantified by titration with sodium hydroxide solution and phenolphthalein indicator.

In the reusability test, the used catalyst was filtered from the reaction mixture, followed by washing with methanol and deionised water. The recovered catalyst was dried in the 80 °C oven until no mass change observed, and it was saved for subsequent reaction cycles. The reaction conditions of the consecutive cycles were the same as the first cycle.

To evaluate the stability of the functional acid species in the hypercrosslinked materials in contact with organic liquids and water, a known amount of pre-dried catalyst was added to a round-bottom flask containing 100 ml of the contacting liquid. The mixture was then stirred for a recorded time after which the acid site concentration of catalyst was also determined by acid-base back titration which was the same as previously stated.

### **2.3. Results with discussion**

#### 2.3.1. Catalyst characterisation

The characteristics of the catalysts are shown in **Table 2.1**. The apparent BET surface areas of the hypercrosslinked Purolite resins are much larger than that of the macroporous resin, Amberlyst 35. The measured BET surface area of the hypercrosslinked polymers is appropriately interpreted as a reflection of their sorption capacity towards nitrogen, because there is no real solid border in the interior of the open-worked hypercrosslinked polymer [3, 4]. Though the surface

area of hypercrosslinked resins is large, the pore volume is relatively small. This would suggest that the majority of the pores are small. Indeed, the hypercrosslinked resins would be expected to contain large amount of micropores introduced by the methylene bridges in addition to meso- or macropores. The intense crosslinking of the polymer chains leads to the formation of swollen gel. When the polymer chains are removed from the solvent, the micropores are retained due to the high rigidity of the polymer network.

Because large quantities of the free aromatic rings in hypercrosslinked polymers have contributed to the crosslinking, the sulfonic acid loading is much lower than that of conventional macroporous polymers. The back titration experiments showed acid site concentrations of 0.98 mmol/g and 2.05 mmol/g for D5081 and D5082 respectively. These data broadly agree with the results estimated from elemental sulfur analysis by Saha et al [5]. Compared to D5081, the higher acid site concentration of D5082 is in line with its lower surface area.

**Table 2.1.** Characteristics of Purolite D5081, Purolite D5082 and Amberlyst 35

Catalyst	Surface area (m <sup>2</sup> /g)	Pore volume (cm <sup>3</sup> /g)	Acid site concentration (mmol/g)	
			Titration <sup>1</sup>	S content
<b>Purolite D5081</b>	588	0.39	0.98	1.25
<b>Purolite D5082</b>	347	0.36	2.05	1.85
<b>Amberlyst 35</b>	52.2	0.35	5.43	-

1. The error was  $\pm 0.05$  mmol/g.

### 2.3.2. Catalytic activity

As seen in **Fig. 2.1**, the two hypercrosslinked catalysts displayed similar activity to Amberlyst 35 in acetic acid esterification with methanol. With oleic acid

esterification with methanol, the activity of Amberlyst 35 was significantly lowered while the activities of the hypercrosslinked catalysts were similar (**Fig.2.2**). The low oleic acid conversion over Amberlyst 35 could be ascribed to its small surface area. The highest conversion of oleic acid was achieved by D5081 due to its highest surface area though its acid site concentration is the lowest. At first thought, the esterification of oleic acid would be much slower than that of acetic acid under the same condition due to the large molecular size. However, this is not the case for hypercrosslinked sulfonic acids D5081 and D5082 catalysis, which indicates that large molecules can access to the acid sites of the hypercrosslinked catalysts. In addition, D5081 is more active than D5082 in the hydrophobic esterification of oleic acid. Considering the large surface area of both hypercrosslinked resins where large molecules would be able to penetrate freely, the faster conversion rate corresponds to the more hydrophobic catalyst which is D5081 [3].

Initial turnover frequencies (TOFs) were calculated from the change in concentration of the carboxylic acid over the first 10 minutes of reaction where the reaction rate appeared constant (**Table 2.2**). It is interesting to find that these hypercrosslinked poly(St-DVB) sulfonic acid catalysts tend to retain a constant hierarchy of intrinsic activity with no dependence on the nature of the carboxylic acids, as can be seen from the finding that the initial TOF ratios of D5082 to D5081 are always 0.37-0.40 in esterification of both acetic acid and oleic acid. If we assume that the acid groups in D5081 are all readily accessible and are equally active, the accessible active sites in D5082 would be approximated to 0.80 mmol/g provided D5082 contains 2.05 mmol/g sulfonic acid groups. Under the same

reaction conditions, Andrijanto et al estimated that a maximum of 0.47 in 4.7 mmol/g acid sites in Amberlyst 15 are accessible to oleic acid and methanol [6]. Compared to this finding, the sulfonic acid functionalisation on the hypercrosslinked polymer network is more effective for catalysis.

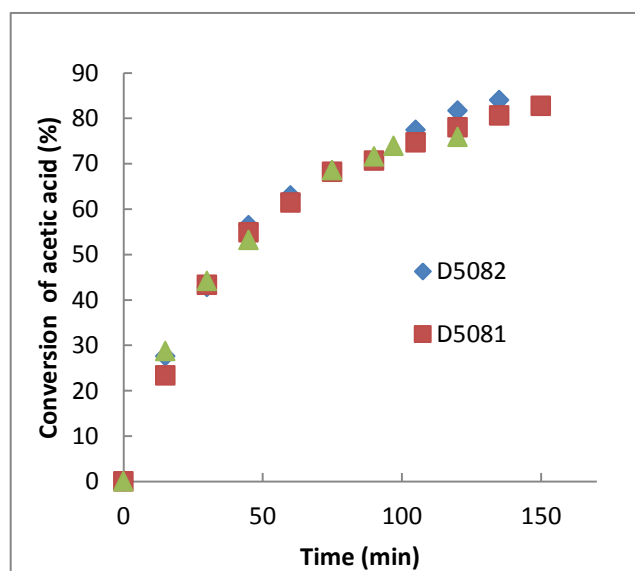


**Fig. 2.1.** Conversion plots of acetic acid with methanol over D5081, D5082 and Amberlyst 35 catalysis (catalyst amount: 0.200 g, acetic acid: 4.00 g, methanol: 20.0 g, temperature: 65 °C, stirring speed: 600 rpm).

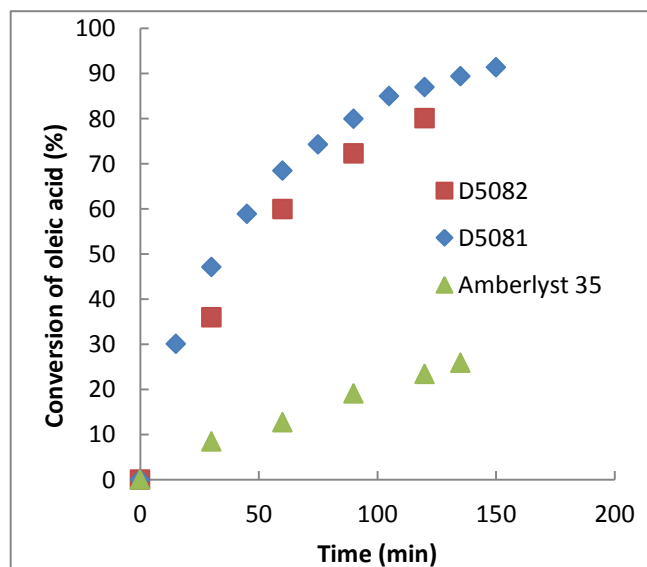


**Fig. 2.2.** Conversion plots of oleic acid with methanol over D5081, D5082 and Amberlyst 35 catalysis (catalyst amount: 0.200 g, oleic acid: 4.0 g, methanol: 20.0 g, temperature: 65 °C, stirring speed: 600 rpm).

**Table 2.2.** Initial TOFs of D5081, D5082 and Amberlyst 35 in the esterification with methanol calculated from acid conversion in the first ten minutes of reactions

Catalyst	Initial TOF ( $\text{min}^{-1}$ ) <sup>1</sup>	
	Acetic acid	Oleic acid
<b>D5081</b>	<b>4.1</b>	<b>0.96</b>
<b>D5082</b>	<b>1.5</b>	<b>0.38</b>
<b>Amberlyst 35</b>	<b>0.72</b>	<b>0.029</b>

1. as with all kinetic measurements, to  $\pm 2\%$

### 2.3.3. Reusability of D5081 and D5082

Five consecutive esterification cycles of 0.40 g acetic acid and 20.0 g methanol were conducted to evaluate the reusability of D5081 and D5082. The reactions were conducted using a stirring speed of 600 rpm and at a temperature of 65 °C for 2 hours after which time the catalyst beads were recovered and activated for the subsequent cycle. The catalytic activity of D5081 decreased steadily from the first cycle to the fifth cycle, while activity D5082 decreased significantly during the first two cycles but remained stable thereafter (**Fig. 2.3**). Above all, deactivation of both catalysts occurred most significantly between the first and the second cycle. Potential causes for such deactivation could be contamination of the pore structure by deposition of organic species, and leaching of acid sites [7, 8]. The potential organic species that would deposit onto the catalyst surfaces are methanol, acetic acid, methyl acetate and water. However these species are unlikely to be retained in catalyst pores due to their sizes or volatility. Thus, the hypothesis proposed here is that the deactivation is due to leaching of the acid sites in D5081 and D5082.

Before each esterification cycle, acid site concentrations of D5081 and D5082 were determined. The acid sites of D5081 decreased steadily from 0.98 mmol/g to 0.31

mmol/g in the first four cycles, whereas the acid site concentration of D5082 was decreased but was retained after the second cycle at about 1.4 mmol/g (**Fig. 2.4**). The trends of decrease in acid site concentrations correlate the behaviour of corresponding 2-h acetic acid conversions. This in part linked the catalyst deactivation to leaching of acid sites. The reason for the leaching was investigated as detailed in the next section.

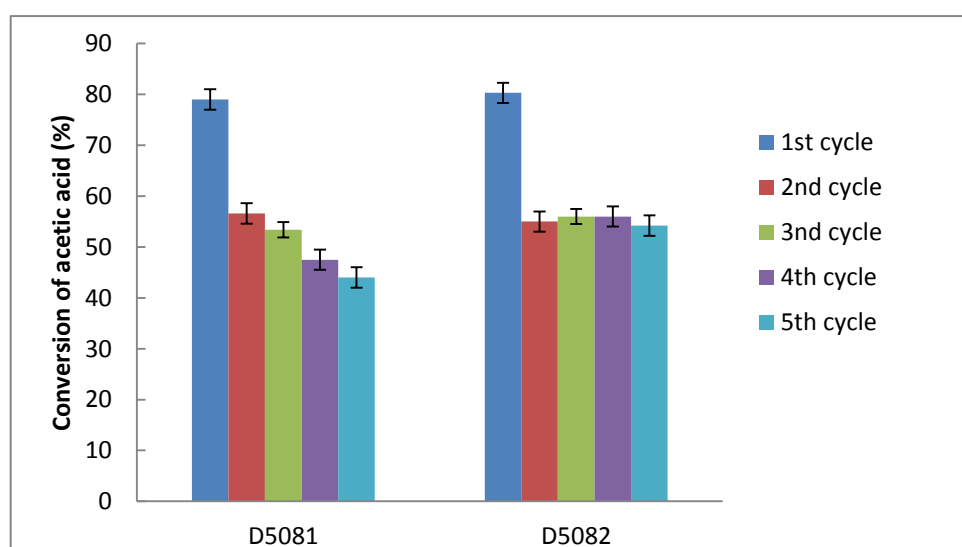


**Fig. 2.3.** Conversion of acetic acid with methanol in 2 hours of five consecutive reaction cycles (catalyst amount: 0.200 g, acetic acid: 4.00 g, methanol: 20.0 g, temperature: 65 °C, stirring speed: 600 rpm). Conversions are estimated to within  $\pm 2\%$  (95% confidence).

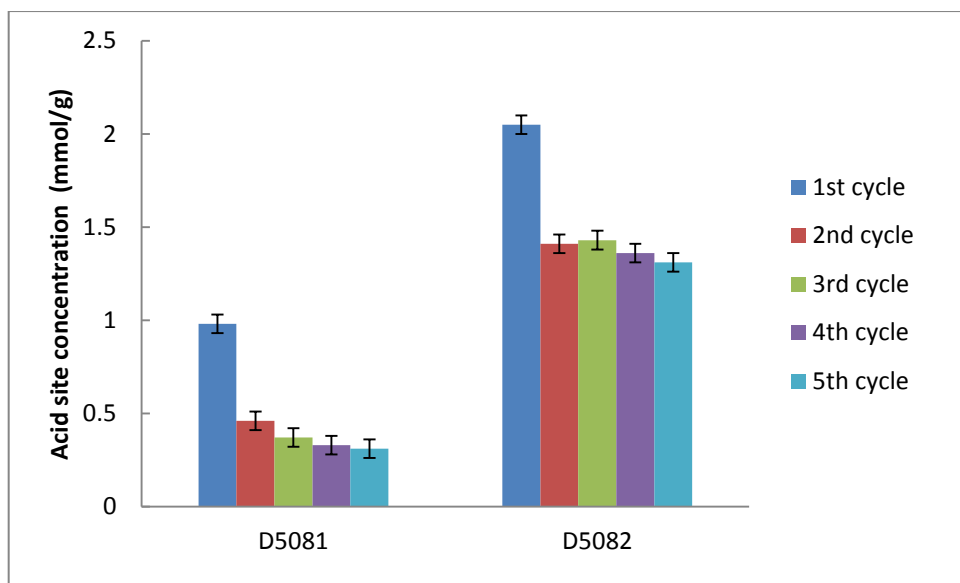


**Fig. 2.4.** Acid site concentrations of D5081 and D5082 determined before each reaction cycle. The errors are to within 0.05 mmol/g.

#### 2.3.4. Acid site leaching of D5081 and D5082 contacted with organic liquids

Though the esterification reaction is initiated by protonation of acetic acid, there is equilibrium of competitive adsorptions on the acid sites between methanol and acetic acid. When a large excess amount of methanol is used, the acid sites are inevitably solvated by methanol. Consequently, the acid sites in D5081 and D5082 might be more prone to leach out in contact with methanol. To test whether methanol is the cause of the acid site leaching, 20.0 g fresh methanol was contacted with 0.200 g activated D5081 for 2 hours and the catalyst was then filtered out. The pre-treated methanol was charged to a reactor to react with 4.00 g fresh acetic acid with no solid catalyst, using the same experimental conditions. A blank experiment of fresh methanol and fresh acetic acid without catalyst was also run. A conversion of 50% fresh acetic acid was observed, whereas the blank reaction only esterified 2.3% of acetic acid in 2 hours, meaning that the autocatalysis of by acetic acid is

minimal (**Fig. 2.5**). Therefore, the high conversion of acetic acid with pre-treated methanol was attributed to homogeneous catalysis by methanol leached acid species from the catalyst.

Additionally, acetic acid was tested to investigate whether it also causes the acid site leaching. Prior to reacting with fresh methanol, 4.00 g pure acetic acid was contacted with 0.200 g D5081 for 2 hours. Later, 35% of pre-treated acetic acid was converted by fresh methanol applying the same reaction condition. Therefore, it was concluded that the acid sites in D5081 can leach out in contact with both methanol and acetic acid.

Generally, the acid groups from the catalyst will form sulfuric acid when they leach to the liquid phase. The intrinsic activity of sulfuric acid accounts on the condition that 1 mol H<sup>+</sup>/1 mol H<sub>2</sub>SO<sub>4</sub> has sufficient acidity to catalyse the reaction [9]. Therefore, the difference in acetic acid conversions from each pre-treated reactant facilitates the comparison of the quantities of acid species that leached to each reactant through pre-treatment. By comparing the homogeneously contributed activities of leached species, 20.0 g methanol could be more effective at causing acid site leaching from D5081 than 4.00 g acetic acid as in the esterification reactions.

Leaching of acid sites of D5081 and D5082 was also observed in other organic liquids that are less polar than methanol and acetic acid. As shown in **Fig. 2.6**, reduced acid site concentrations of 0.72 mmol/g and 0.88 mmol/g were found in D5081 after 2-hour contact with toluene and methyl acetate at 65 °C respectively,

while the according values for D5082 were 1.49 mmol/g and 1.80 mmol/g. The acid site concentrations were unchanged for both D5081 and D5082 in contact with heptane under the same conditions for 2 hours, although a small decrease is evident for D5082 depending upon error bars. These reveal that the acid sites of both D5081 and D5082 only tend to leach out in polar liquids.

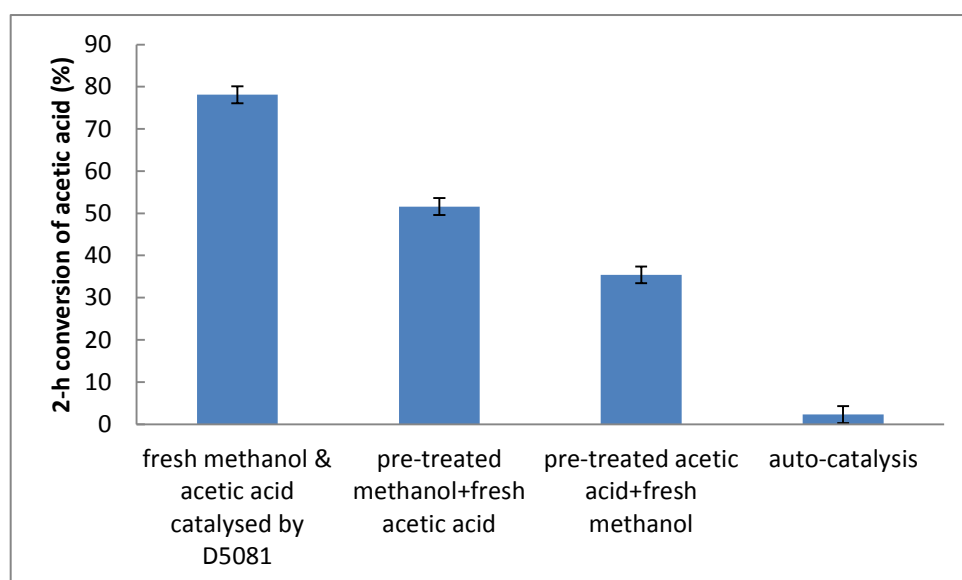


**Fig. 2.5.** Study on homogeneous contribution of D5081 and non-catalysed esterification of acetic acid (catalyst amount: 0.200 g, acetic acid: 4.0 g, methanol: 20.0 g, temperature: 65 °C, stirring speed: 600 rpm). Conversions are estimated to within  $\pm 2\%$  (95% confidence)

When in contact with liquids, the hypercrosslinked poly(St-DVB) sulfonic acids undergo hydrophobic/hydrophilic interaction. Functionalisation with highly hydrophilic sulfonic groups would increase their tendency toward solubility in polar media through hydrogen bonding [10]. When the hypercrosslinked poly(St-DVB) sulfonic acids are in contact with hydrophobic liquids such as heptane, the interaction is absent so acid site leaching was not observed. In addition, the faster rate of leaching in toluene is not surprising, because toluene, though not so

hydrophilic, would accelerate the polymer decomposition because it structurally resembles the styrene unit of hypercrosslinked poly(St-DVB) moieties [11].

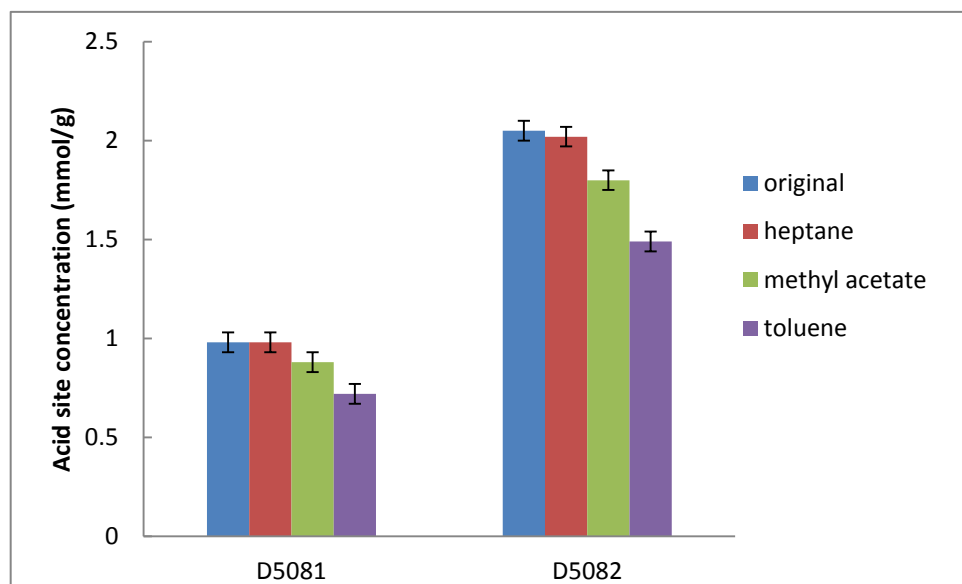


**Fig. 2.6.** Acid site concentration of D5081 and D5082 after treatment with various liquids at 65 °C for 2 hours. The error is 0.05 mmol/g.

### 2.3.5. Origin of the leachable acid species

The acid species detected in the hypercrosslinked poly(St-DVB) catalysts would be of two forms. One is the chemically bonded sulfonic acid groups on the catalyst surface. The other one is sulfuric acid trapped in the catalyst pores. To find out the origin of the leachable species, water was chosen as the contacting medium instead of any organic liquids on the basis that water is a better solvent for simple acid species. Evaluation of the leaching behaviour in water is also important, because hypercrosslinked resins and the sulfonated forms might well be used as sorbents for water purification [12-14]. To conduct this evaluation, 0.20 g dried D5081 was charged to a flask containing 100 ml deionised water. The mixture was sealed at 20 °C and stirred at 600 rpm. The remaining acid concentration of D5081 was

monitored as a function of time until the leaching stopped. The results show that 0.30 mmol acid sites per gram of D5081 were lost in the first 5-hour treatment and the permanent acid concentration of 0.45 mmol/g was obtained on extensive treatment for 233 hours (**Fig 2.7**). The 0.01 mmol/g difference between 233 hours and 305 hours is regarded as negligible. Therefore it was concluded that acid site leaching would cease and that about 45% of original acid sites could permanently remain in the D5081 beads in contact with water at 20 °C. For comparison, Amberlyst 35 was treated with deionised water by applying the same method. 5.09 from a total 5.43 mmol/g acid sites were permanently remained after 67 hours of the experiment, which indicates acid site leaching was minor in Amberlyst 35. D5082 was also treated with water following the same method. After 5-hour interaction, most of the D5082 beads decomposed; hence further quantitative analysis for D5082 could not be conducted.

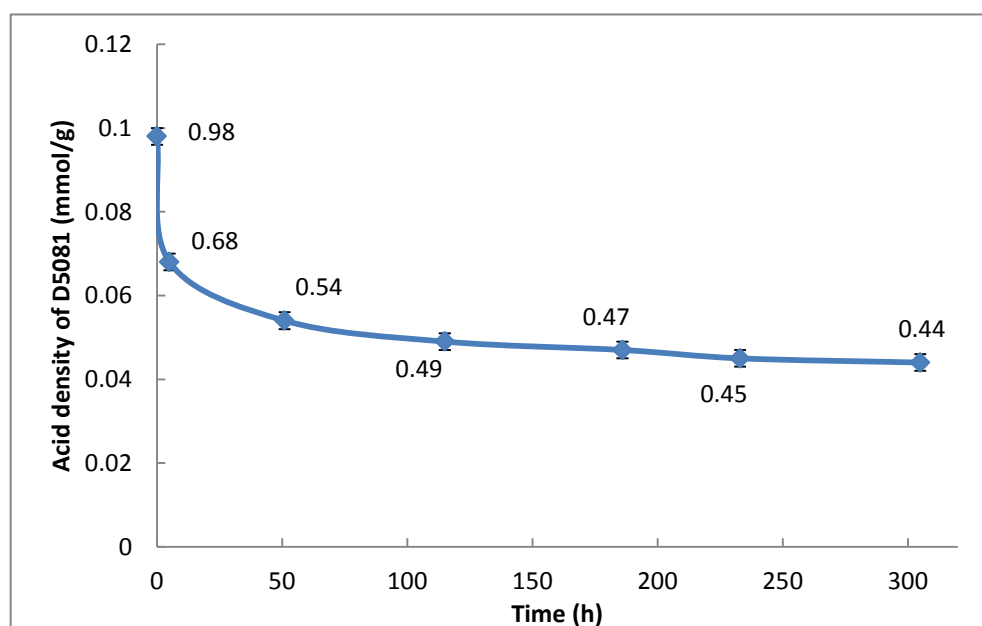


**Fig. 2.7.** Plot of remaining acid sites of D5081 treated with water at 20 °C stirred at 600 rpm. The errors were controlled within 0.02 mmol/g.

To find out the origin of leachable species from D5081, the effect of temperature on the leaching of acid sites of D5081 in water was investigated. Assuming the leaching process follows first-order kinetics in terms of the sulfonic acid groups, the rates of acid site leaching were calculated from the decrease in acid site concentration of D5081 in contact with water for 5 hours (**Table 2.3**). It was found that the rate of acid-site leaching can be roughly described by the Arrhenius Law. From **Fig. 2.8**, the activation energy was calculated to be 9.4 kJ/mol. In general, the activation energy is about 40 kJ/mol for a reaction catalysed by sulfonic acid, while it is 4-12 kJ/mol for a diffusion-controlled process [15, 16]. The low activation energy for the leaching process suggests the leaching of acid sites from D5081 is more likely to resemble the diffusion process of a species through the polymeric networks, which, in other words, implies that the majority of the leached species from D5081 are trapped or weakly bonded sulfuric acid rather than chemically bonded sulfonic acid groups. The ease of leaching of entrained sulfuric acid means D5081 and D5082 are less effective catalysts. In addition, the use of hypercrosslinked networks as sorbents in aqueous media also requires caution, because the hypercrosslinked polymer/water interaction would potentially cause hypercrosslinked network deformation as was observed in the case of D5082.

**Table 2.3.** Temperature dependence of acid site loss in the first 5-hour contact with water and activation energy of the leaching mechanism

Temperature / °C	(T)	Acid site loss from 1g D5081 / mmol	Rate of leaching (k) / mmol/(gh)	Activation energy (E <sub>a</sub> ) / kJ/mol
20		0.30	0.059	9.6 ± 1.4
40		0.39	0.079	
65		0.47	0.093	
90		0.65	0.130	

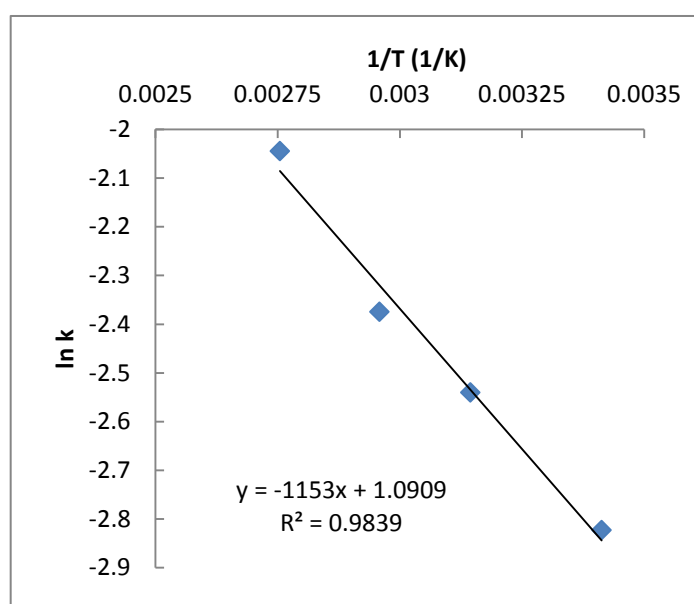


**Fig. 2.8.** Arrhenius-van't Hoff plot on the acid site loss of D5081 in contact with water for 5 hours.

## 2.4. Summary of results

This chapter describes a study of the catalytic performance and leaching of acid sites in two commercially available hypercrosslinked poly(St-DVB) sulfonic acids D5081 and D5082. The results are summarised as following:

- In acetic acid esterification, the hypercrosslinked resins Purolite D5081 and D5082 are as active as macroporous Amberlyst 35.

- In oleic acid esterification, Purolite D5081 and D5082 are more active than Amberlyst 35.
- The high activities of D5081 and D5082 are facilitated by large surface area and high accessibility of acid sites to the reactants.
- The trend of catalytic deactivation of D5081 and D5082 is related to the decreased acid site concentrations of these two catalysts.
- The acid sites of D5081 and D5082 partly leach out in contact with polar organic liquids.
- The acid sites of D5081 partly leach out in the contact with water, and permanent acid site concentration can be obtained.
- The activation energy calculated from Arrhenius-van't Hoff plot suggests the leachable species from D5081 to water is mainly trapped sulfuric acid.

## References

- [1] G. D. Yadav and P. H. Mehta, *Ind. Chem. Res.*, 33 (1994) 2198-2208.
- [2] J. Otera, *Esterification: Methods, Reactions and Applications*, Wiley-VCH, Weinheim, 2003.
- [3] M. P. Tsyurupa and V. A. Davankov, *React. & Funct. Polym.*, 53 (2002) 193-203.
- [4] M. P. Tsyurupa and V. A. Davankov, *React. Funct. Polym.*, 66 (2006) 768-779.
- [5] S. Z. Abidin, K. F. Haigh and B. Saha, *Ind. Eng. Chem. Res.*, 51 (2012) 14653-146645.
- [6] E. Andrijanto, E. A. Dawson and D. R. Brown, *Appl. Catal. B: Envir.*, 115 (2012) 261-268.
- [7] K. Kumbilieva, L. Petrov, Y. Alhamed and A. Alzahrani, *Chin. J. Catal.*, 32 (2011) 387-404.
- [8] C. H. Bartholomew, *Appl. Catal. A: Gen.*, 212 (2001) 17-60.
- [9] J. M Marchetti and A. F. Erruzu, *Biomass. & Bioen.*, 32 (2008) 892-895.
- [10] X. Mo, D. E. Lopez, K. Suvannakarn, Y. Liu, E. Lotero, J. G. Goodwin Jr., C. Lu, *J. Catal.*, 254 (2008) 332-338.
- [11] A. V. Pastukhov, V. A. Dvankov, E. V. Sidorova, E. I. Shkol'nikov and V. V. Volkov, *Russ. Chem. Bull., Int. Ed.*, 56 (2007) 484-493.
- [12] B. Li, F. Su, H. Luo, L. Liang and B. Tan, *Micro. & Meso. Mater.*, 138 (2011) 207-214.
- [13] M. P. Tsyurupa, M. M. Ilyin, A. I. Andreeva, and V. A. Davankov, *J. Anal. Chem.* 352 (1995) 672-675.
- [14] V. V. Azanova and J. Hradil, *React. & Funct. Polym.*, 41 (1999) 163-175.
- [15] E. A. Abdel-Aal, *Hydrometallurgy*, 55 (2000) 247-254.
- [16] M. A. Jackson, I. K. Mbaraka and B. H. Shanks, *Appl. Catal. A: Gen.*, 310 (2006) 48-53.

## Chapter 3

# Preparation, Characterisation and Activity of Home-made Hypercrosslinked Poly(St-DVB) Sulfonic Acids

### 3.1. Introduction

The acid sites in Purolite D5081 and D5082 tend to leach out in contact with polar liquids. The leaching of acid sites in D5081 is mainly due to the presence of trapped sulfuric acid. An extensive wash of D5081 with water resulted in leaching of more than half of the total acid sites, while the D5082 polymeric structure tended to rapidly decompose in contact with water. These properties mean that D5081 and D5082 are potentially less effective catalysts. To test the catalytic activity in esterification of carboxylic acids, robust hypercrosslinked sulfonic acids are required. Therefore, in this chapter, a series of hypercrosslinked polymer supported sulfonic acids were prepared on the hypercrosslinked poly(St-DVB) support of commercially available MacroNet 200 (MN 200). Two different sulfonation routes were applied in order to achieve high degrees of sulfonation. After the samples were successfully sulfonated, they were thoroughly washed to remove trapped sulfuric acid. The washed samples were then characterised in terms of acid site concentration, surface area and porosity. The commercially available MacroNet 500 (MN 500) which is directly sulfonated from MN 200 was also characterised for comparison. In addition, one of the prepared samples M2E, along with Amberlyst 15, D5081 and MN 200,

was sent for solid-state NMR analysis to identify the structural differences of these materials and to check whether the methylene bridges of the hypercrosslinked network are affected by functionalisation with sulfonic acid. Finally, the performances of the prepared hypercrosslinked poly(St-DVB) sulfonic acids and MN 500 were compared for the esterification of acetic acid with methanol. The activities and reusability of these materials were compared.

## **3.2. Experimental**

### 3.2.1. Materials

MN 200 and MN 500 were supplied by Purolite Int. Ltd. UK. Amberlyst 15 and 35 were provided by Rohm & Haas France S.A.S. Dichloromethane (99.8+ %) and chloroform (99.8+ %) were purchased from Fisher Scientific, UK. Sulfuric acid (98 wt. % & 95 wt. %) and silver sulfate were provided by Sigma Aldrich.

### 3.2.2. Sulfonation procedure

MN 200 was sulfonated using two different routes. Route 1 applied concentrated sulfuric acid over a silver sulfate catalyst [1, 2], and Route 2 used in-situ synthesised acetyl sulfate as the sulfonation reagent [3].

#### 3.2.2.1. Route 1

The MN 200 beads were sulfonated to M2A in a 200 ml three-necked, round-bottomed flask equipped with a magnetic stirrer and reflux condenser. 100 ml of sulfuric acid (98%) was loaded to the flask, stirred at 600 rpm and was heated to

75 °C. 0.02 g silver sulfate was charged to the flask. After the solids were dissolved, the MN 200 beads (wet, 2.5 g), previously swollen in 30 ml chloroform for 24 hours at 20 °C, were slowly added to the flask. After the mixture was kept for 24 hours, the reaction was quenched by pouring it into a beaker placed in an ice-cool water bath. When it was cooled down, the mixture was diluted by drop-wise addition of deionised water. Then it was filtered in Buchner funnel to recover the solid phase.

M2B was sulfonated using the same procedure, except that MN 200 beads were swelled with Dichloromethane for 3 hours. M2E was prepared with 95 wt. % sulfuric acid with the remaining conditions being the same as that for M2A.

#### 3.2.2.2. Route 2

Acetyl sulfate was synthesised in-situ by adding 10 ml 95 wt. % sulfuric acid to a solution of 20 ml acetic anhydride and 30 ml dichloromethane in an isolated flask in an ice-cool water bath with vigorous stirring for 1 hour.

In another round-bottom flask, 2.50 g dried MN 200 was swollen in 30ml Dichloromethane at 40 °C with stirring speed of 600 rpm for 3 hours. The swollen MN 200 beads were filtered and were immersed in the prepared acetyl sulfate at 45 °C for 3 hours. The reaction was quenched by slowly adding ice-cooled deionised water. Later, the sulfonated beads were separated by filtration and were washed with methanol and deionised water. This sample was named M2C.

To synthesise M2D, 2.50 g MN 200 beads were kept in 20 ml chloroform for 3 hours, and were filtered out before they were sulfonated in 20 ml sulfuric acid, 20 ml acetic anhydride and 5 ml chloroform. The temperature was maintained at 60 °C, and the sulfonation process was kept for 24 hours.

### 3.2.3. Post-treatment of the samples

The prepared samples were washed with methanol and dried for 24 hours at 80 °C in an oven at ambient pressure. 2.0 g dried samples were then washed in 100 ml deionised water for 8 hours (stirred at 300 rpm at room temperature), and the pH of the washing solution was measured with Jewry 3080 pH meter. Then the beads were filtered out and were washed again. These washing steps were repeated several times until the pH value reached 4.0. Because the acid species in the polymers would leach out in water continuously, obtaining neutral washing solution is not always possible after each long time wash. The threshold of pH=4.0 was chosen so that the leached amount of acid in 8 hours was reduced to 0.005 mmol/g on the basis of dried sample. After washing, they were filtered to remove powdered particles, and were dried. After this treatment, the samples can be regarded as free of leachable sulfuric acid.

### 3.2.4. Acid site concentration

In Chapter 2, acid site concentration was determined by back titration, which needed to be conducted several times to obtain repeatable results. In this chapter, the concentrations of acid sites of the samples were determined by aqueous titration

with sodium hydroxide solution after cation exchange with sodium ions from 1.0 mol/L NaCl solution. The cation exchange was carried out using the pressurised reactor Autoclave Engineers Magnedrive III for 7 hours. This time was tested as sufficient for complete ion-exchange for the acid sites. The ion-exchange condition was set as 1.5 times ambient pressure at 85 °C with a stirring speed of about 2000 rpm. By using this method, the errors of the measured acid site concentrations of the catalysts were controlled within 0.03 mmol/g

Conducting a complete cation-exchange in the batch reactor at low temperature requires quite a long time (usually over 24 hours), while the cation-exchange at high temperature is inevitably accompanied by vaporisation of the solution, which leads to inaccurate results. The use of pressurised reactor enables the cation-exchange to be conducted at higher temperature with shortened time; and vaporisation is prevented by sealing the catalyst-solution mixture in the reactor vessel.

#### 3.2.5. Surface area and porosity measurement

Nitrogen porosity measurements were conducted on the bead samples using the Micromeritics ASAP 2020. Surface areas were calculated by the BET method. Desorption isotherms were used to calculate pore volume and average pore width with the BJH method.

### 3.2.6. Solid-state NMR

The solid-state  $^1\text{H}$  and  $^{13}\text{C}$  NMR experiments were conducted by the EPSRC National Solid-state NMR Service at Durham University.

The solid-state  $^1\text{H}$  NMR spectra were recorded on a Varian VNMRS 400 spectrometer referencing to neat tetramethylsilane. The measurements were carried out with a direct excitation technique. The spectral width was 40 kHz, the frequency was 400 MHz with a spin-rate of 14 kHz. In  $^1\text{H}$  NMR analysis for the samples swollen in DCM, the spectral width was 100 kHz, the frequency was 100 MHz, and the spin-rate was 4050 Hz.

The solid-state  $^{13}\text{C}$  spectra were recorded on the same spectrometer operating at 100.562 MHz for  $^{13}\text{C}$  nuclei with a spin rate of 14 kHz. Neat tetramethylsilane was used as the external standard. Qualitative information was obtained using cross polarisation technique, which was applied to enhance the method sensitivity. In this experiment, the contact time was 3 ms, repetition numbers were 2016-3936, and repetition period was 2 s.

### 3.2.7. Catalytic activity and reusability

The test for catalytic activity and reusability of the prepared catalysts for esterification of acetic acid with methanol applied the same reaction conditions as those described in Chapter 2 except that the reaction temperature was changed to 60 °C. The change of temperature from 65 °C to 60 °C was enacted to reduce

vaporisation of the methanol during the reaction. At the stirring speed of 600 rpm, the external mass transfer resistance was also eliminated. The catalyst recovery from the reaction mixture also followed the same procedure described in Chapter 2.

### **3.3. Results and discussion**

#### 3.3.1. Product yield and acid site concentration

The samples were prepared from MN 200 in the presence of DCM which swelled the polymer matrix to expose the internal pores to sulfuric acid. Introducing the sulfonic acid groups generated mechanical tension within the polymer that broke the polymeric beads, which led to low yields of sulfonated samples (**Table 3.1**). Additionally, long-time contacting with swelling agent caused severe bead breaking. This was evidenced by less than 10% of M2A being obtained from swelling for 24 hours with DCM. However, it seems that altering the swelling agent did not affect the sulfonation level because M2B and M2E, which were sulfonated in DCM and chloroform respectively, exhibit similar acid site concentration. From the similar yield and acid concentration of M2B, M2D and M2E, it is also likely that the two sulfonation routes are equally effective. From safety considerations, sulfonation with in-situ synthesised acetyl sulfate would be more advantageous because it applied a lower reaction temperature and dilute reagents were used. Nevertheless, applying either sulfonation route, some products were less successfully sulfonated. M2C with a low acid site concentration was obtained due to the low temperature (45

°C) and short reaction time applied (3 hours). The quantity of M2A obtained was not adequate and the reason was not clear, so it was not suitable for further analysis.

**Table 3.1.** The percentage yield and acid site concentration of the sulfonated samples

	<b>M2A</b>	<b>M2B</b>	<b>M2C</b>	<b>M2D</b>	<b>M2E</b>
<b>Yield (wt. %)</b>	<10	81	22	79	80
<b>Acid conc. (mmol/g)<sup>1</sup></b>	-	0.77	0.42	0.74	0.78

1. Error:  $\pm$  0.03 mmol/g.

### 3.3.2. Surface area and porosity

**Figs. 3.1** and **3.2** show the nitrogen adsorption and desorption isotherms of four home-made hypercrosslinked poly(St-DVB) sulfonic acid resins and two commercially available hypercrosslinked poly(St-DVB) resins, MN 200 (unsulfonated) and MN 500 (sulfonated on MN 200). It can be seen that the adsorptions are of Type II according to the IUPAC classification [4]. The isotherm plots of the sulfonated resins are almost parallel to that of MN 200 at high pressure beyond  $p/p_0 = 0.1$ , indicating sulfonation did not apparently change the porous structure [5]. The progressive functionalisation with sulfonic acid reduced the measurable surface area and total pore volume (**Table 3.2**). This may be a result of acid groups, solvated acid groups that block some of network of pores in the hypercrosslinked structure. The values of average pore width are just above the micropore region. Progressive sulfonation seems not to significantly distort the average pore width.

**Table 3.2.** Properties of various hypercrosslinked poly(St-DVB) sulfonic acids

Hypercrosslinked resins	MN 200	M2C	M2D	M2B	M2E	MN 500
BET surface area <sup>1</sup> (m <sup>2</sup> /g)	687	657	519	522	458	424
Total pore volume <sup>2</sup> (cm <sup>3</sup> /g)	0.442	0.376	0.307	0.303	0.276	0.250
Average pore width <sup>3</sup> (nm)	2.61	2.33	2.41	2.38	2.47	2.44
Acid site conc. (mmol/g) <sup>4</sup>	0	0.42	0.74	0.77	0.78	1.20

1. Measured by single point BET method at  $P/P_0=0.20$ ,
2. Pores less than 65 nm width by single point adsorption at  $P/P_0=0.97$ ,
3. Adsorption average pore width (4V/A by BET),
4. Error:  $\pm 0.03$  mmol/g.

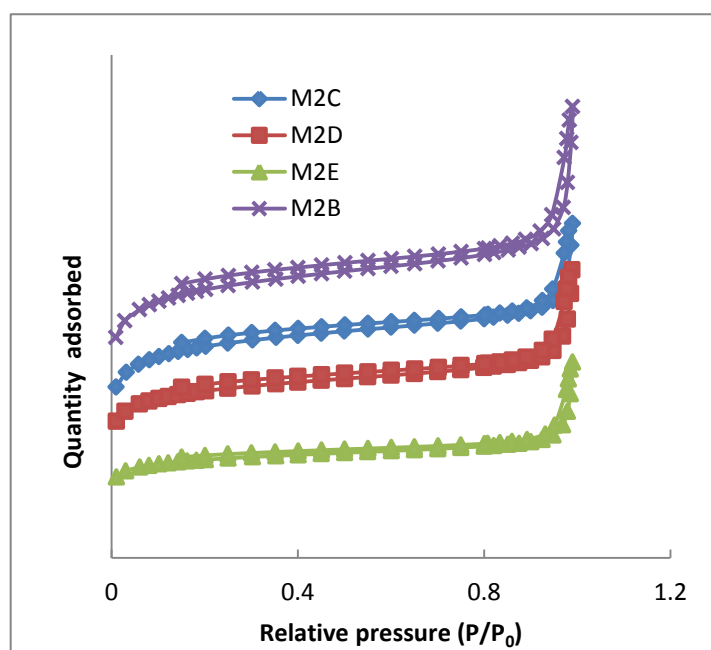


**Fig. 3.1.** N<sub>2</sub> adsorption-desorption isotherms of home-made hypercrosslinked poly(St-DVB) sulfonic acids. The y-scales (quantity adsorbed) are offset for clarity.

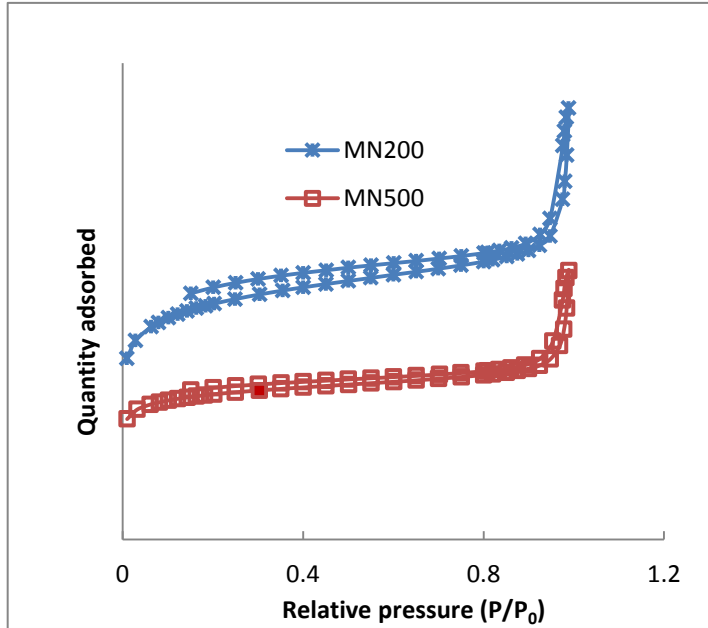


**Fig. 3.2.** N<sub>2</sub> adsorption-desorption isotherms of commercially available MN 200 and MN 500. The y-scale (quantity adsorbed) is offset for clarity.

**Figs. 3.3** and **3.4** show the four curves of pore volume over pore width of M2E within the pore width range of 1.7 -180 nm. Two pore volume plots were differentiated over the pore width, and the other two plots were differentiated from logarithm of pore width. For each pair of plots, the pore volumes were calculated from both desorption branch and adsorption branch of the hysteresis loop. One similarity of the four plots is the broad and unsymmetrical pore size distributions (PSDs) which result from the bimodal porosity of the hypercrosslinked materials. It seems, however, the calculation of PSD of the hypercrosslinked polymers from different manners generated contradictory impressions of their porous structures. Normally, if pores are comprised of independent capillaries, the use of the desorption branch is applicable. The adsorption branch of the hysteresis loop is better fitted for pore size distribution calculation of bottle-like pores because liquid

in the narrow capillaries prevents evaporation of the condensate from larger compartments [7]. The curves from  $dV/dw$  and  $dV/d\log(w)$  methods show small difference, while the information of pore sizes seems ambiguous judging from the  $dV/d\log(w)$  plots. For comparison, the desorption branch of the nitrogen sorption isotherm using  $dV/dw$  method was chosen for the calculation of the pore size distribution of the sulfonated samples and their polymer support MN 200 (**Fig. 3.5**). The pore volumes were decreased with the increase of the amount of supported sulfonic acid. It seems that incorporating sulfonic acid preferably affected smaller pores with width less than 10 nm, which again might suggest that sulfonation preferentially occurred at the internal surface of the polymer where the majority of the smaller pores are located.

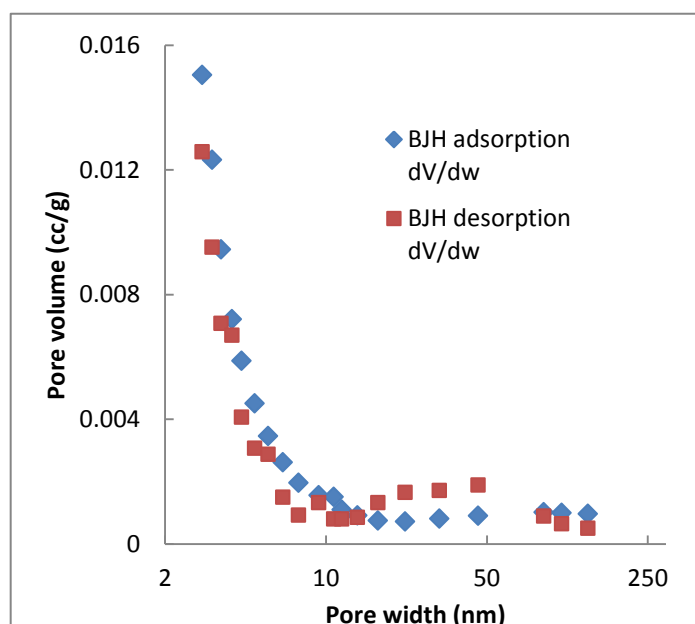


**Fig. 3.3.** Pore size distribution of M2E calculated with  $dV/dw$  method. The pore widths in this figure are presented in non-linear scale for clarity.

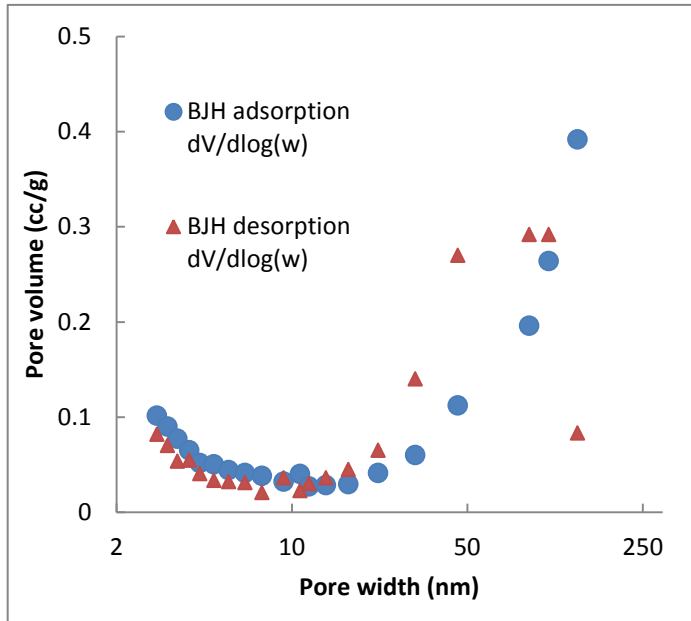


**Fig. 3.4.** Pore size distribution of M2E calculated with  $dV/d\log(w)$  method. The pore widths in this figure are presented in non-linear scale for clarity.

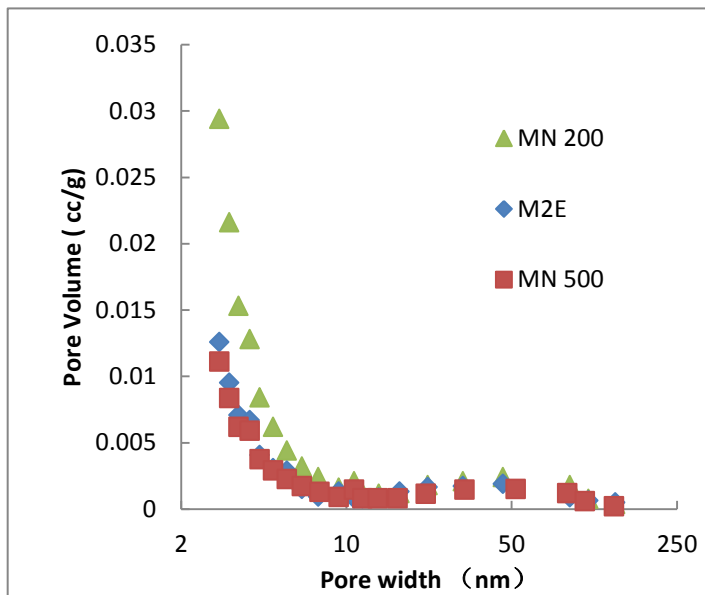


**Fig. 3.5.** Plots of pore size distribution of MN200, MN500, M2C and M2E calculated from the desorption branch of the isotherm using  $dV/dw$  method. The pore widths in this figure are presented in non-linear scale for clarity.

### 3.3.3. Solid-state NMR

Due to the large hydrogen content, hypercrosslinked resins can be analysed by  $^1\text{H}$  NMR spectroscopy. The spectra of D5081, M2B, MN200 and Amberlyst 15 are shown in **Fig. 3.6** with poor resolution (at the end of this chapter). The appearance of Amberlyst 15 spectrum is fundamentally different from those of the other three samples. For Amberlyst 15, the signals at the range of 0-4.00 ppm are typical of aliphatic protons, and the signal at 10.5 ppm is characteristic for aromatic protons [8]. For hypercrosslinked samples, the resolution of spectra is much poorer. Although the exact assessment could not be made because of the broad peaks, it is still clear that the band for aromatic protons shifted from 6.8 ppm downwards to 8.4 ppm when MN200 was converted to M2B. This is an indication of the presence of sulfonic acid groups in M2B, because  $-\text{SO}_3\text{H}$  is an electron-withdrawing group that would make its surrounding protons more electron-poor and the signal was hence deshielded. When the samples were swollen in  $\text{CDCl}_3$ , slightly better resolution was achieved (**Fig. 3.7**, at the end of this chapter). The spectrum of swollen MN200 differs much from the original spectrum, which might reveal there was stronger interaction between MN200 polymer network and  $\text{CDCl}_3$ . The deshielding of the aromatic band of M2B again confirms the successful sulfonation. From the spectrum of swollen M2B, side reaction was detected. The decrease in the band area for aliphatic protons demonstrates that the aliphatic chains would be partly oxidised due to interaction with the strong acidic and oxidative sulfonation medium [6, 9].

Two sets of characteristic bands are identified in the solid-state  $^{13}\text{C}$  NMR spectra of D5081, M2B, MN200 and Amberlyst 15 (**Fig. 3.8**, at the end of this chapter). The bands at about 40 ppm related to aliphatic carbons while the bands at 128 ppm correspond to aromatic carbons [10]. The sulfonated carbon in Amberlyst 15 is easily identified because the corresponding signal was shifted to 149 ppm from other aromatic bands. It is also interesting to note that MN 200 gives a line at 64 ppm. This would be due to the presence of a portion of oxygen-containing groups formed during the steam stripping after the bridging process of the hypercrosslinked polymers [6]. However, one of the purposes is to see whether the methylene bridges in hypercrosslinked MN 200 was affected by sulfonation. The same peak position and the almost equivalent integrated band areas of aliphatic bands of MN200 and M2B do not make it apparent whether the methylene bridges were oxidised or sulfonated, because the signal of the methylene carbons of the crosslinks occurs at 40-50 ppm and is masked by the backbone methane and methylene carbon signals [11].

#### 3.3.4. Catalytic activity and reusability

The home-made M2C, M2D and M2E were used as the catalysts in the testing of acetic acid esterification with methanol. M2B was not tested. MN 500 and Amberlyst 35 were used for activity comparison. From the kinetic profiles, the order of activity is  $\text{MN500} > \text{M2D} \sim \text{Amberlyst 35} > \text{M2E} \gg \text{M2C}$  (**Fig 3.9**). M2D and M2E, exhibiting lower acid site concentration, are still as active as Amberlyst 35. Within the

hypercrosslinked sulfonic acids, the relative activity is in line with their relative order of acid site concentration which is  $MN\ 500 > M2D \sim M2E > M2C$ . However, much higher acid site concentration in MN 500 seems not to highly enhance its activity compared to M2D and M2E. This would suggest the amount of acid sites in M2D and M2E (about 0.78 mmol/g) would be sufficient for catalysing esterification of acetic acid with methanol under these conditions. On the contrary, a much higher proportion of acid groups are built to the macroporous polymeric resins, but the “over-sulfonated” Amberlyst 35 did not exhibit better activity than the hypercrosslinked catalysts. It is likely that Amberlyst 35 is not capable to fully render the acid sites accessible to methanol and acetic acid, because the flexible network of Amberlyst 35 could allow the polar sulfonic acid groups to aggregate hence the acid sites may be shielded by the polymer chains [12]. In the hypercrosslinked poly(St-DVB) sulfonic acids, acid sites are loosely distributed in the highly crosslinked open-work polymers that preserve the ability to restrict their structural configuration. Being free of hindrance, the acid sites are readily accessible to the reactants, which led to a higher reaction rate.

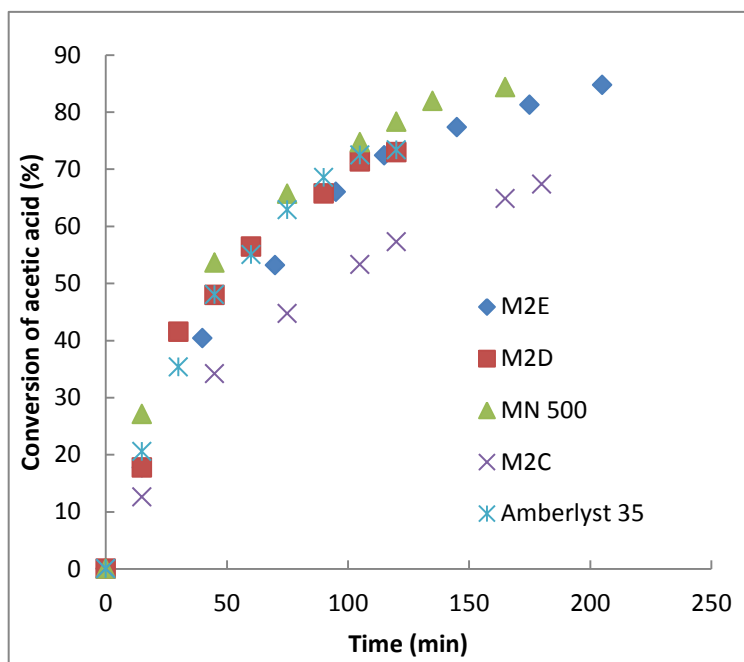


**Fig. 3.9.** Conversion of acetic acid with methanol in the batch reactor catalysed by various catalysts (methanol: 20.0 g, acetic acid: 4.0 g, catalyst: 0.200 g, temperature: 60 °C. stirring speed: 600 rpm).

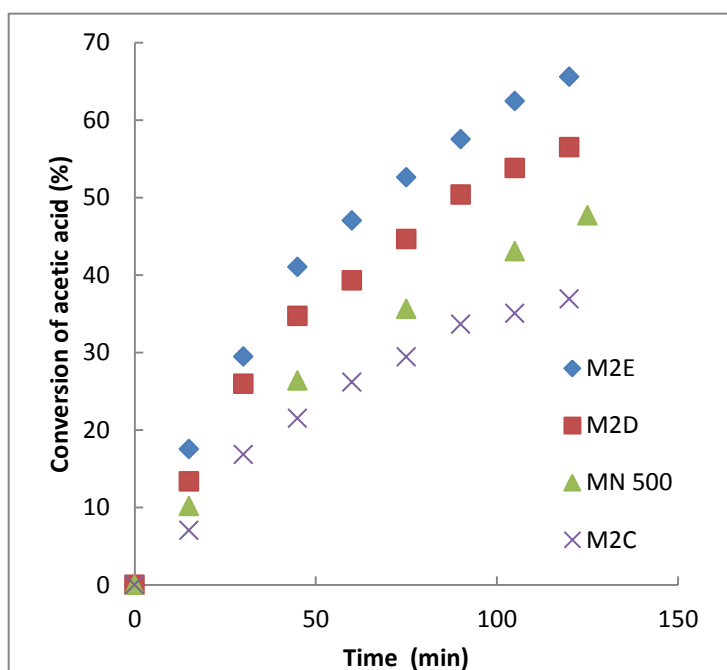


**Fig. 3.10.** Kinetic plots of acetic acid conversion on the four hypercrosslinked catalysts that were recycled from the first esterification cycle (methanol: 20.0 g, acetic acid: 4.00 g, catalyst: 0.200 g, temperature: 60 °C. stirring speed: 600 rpm).

Considering the home-made hypercrosslinked poly(St-DVB) sulfonic acids would suffer from deactivation similar to that of D5081 and D5082, reusability tests for these home-made hypercrosslinked catalysts were conducted. **Fig. 3.10** shows kinetic plots of the four hypercrosslinked catalysts that are in the second reaction cycle of acetic acid with methanol under the same conditions as the first cycle. The activity order of the catalysts is changed to M2E>M2D>MN500>M2C, which suggests deactivation of catalytic performance occurred to different extents for each catalyst. For example, the conversion of acetic acid over MN 500 in the first 2 hours decreased from 78.3% to 47.7% for this catalyst on going to the second reaction cycle, while it decreased from 73.1% to 56.5% for M2D (**Fig. 3.11**). Comparing the relative conversion of acetic acid on each catalyst between the first cycle and the second cycle, it is reasonable to rank M2E>M2D>M2C>MN500 in terms of their retention of activity. After the second cycle, the catalysts were recovered from the reaction mixture, and their acid site concentrations were determined after washing and drying. The results are shown in **Fig. 3.12** along with their initial acid site concentration before the first cycle. The lowered acid site concentrations after second cycle more or less suggest that the home-made hypercrosslinked poly(St-DVB) sulfonic acids were also subject to acid site leaching. The acid site concentrations of MN500 and M2C were decreased from 1.20 to 0.84 mmol/g and from 0.41 to 0.29 mmol/g respectively. The acid concentrations of M2E and M2D were decreased from 0.79 to 0.76 mmol/g and from 0.72 to 0.56 mmol/g respectively. Since it was claimed that possible trapped sulfuric acid was removed

from the prepared catalysts, the acid sites lost here were truly due to the leaching of sulfonic acid groups that were chemically bonded to the polymer supports.

As can be seen in **Figs. 3.11** and **3.12**, the activity loss and acid site leaching of M2E were marginal compared to those of M2C and M2D. This finding leads to the consideration that the different sulfonation routes would affect the stability of sulfonic acid groups functionalised on hypercrosslinked poly(St-DVB), because M2E was sulfonated with concentrated sulfuric acid while M2C and M2D were prepared with in-situ synthesised acetyl sulfate. Though sulfonation with in-situ synthesised acetyl sulfate is milder and safer; sulfonation in concentrated sulfuric acid would be able to reduce leaching of functionalised groups, and hence produce hypercrosslinked poly(St-DVB) sulfonic acid catalysts which are more robust.

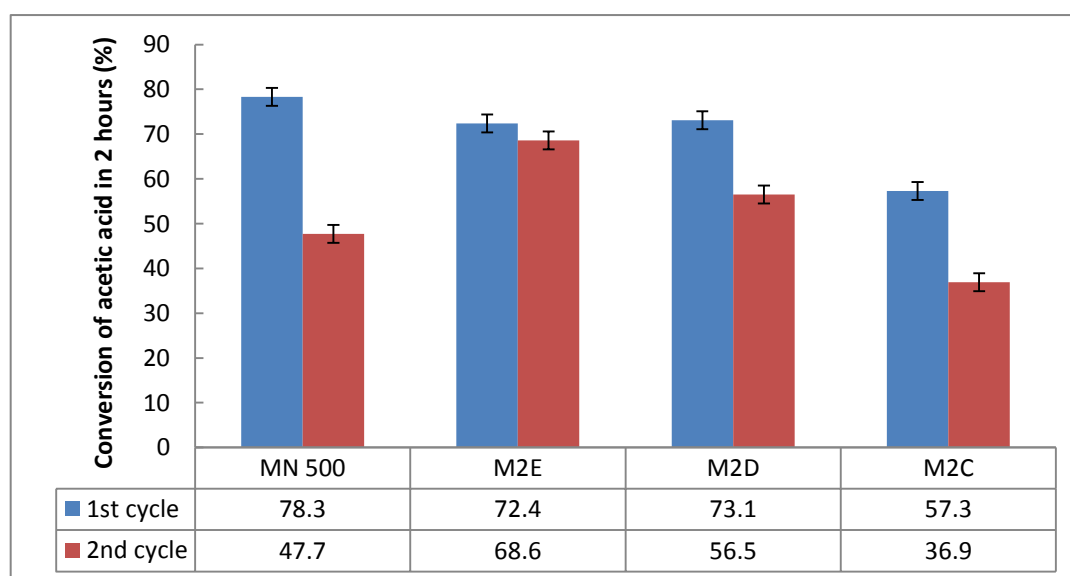


**Fig. 3.11.** Comparison of acetic acid conversion on the four hypercrosslinked catalysts in the first reaction cycle and the reuse cycle (methanol: 20.0 g, acetic acid: 4.00 g, catalyst: 0.200 g, temperature: 60 °C. stirring speed: 600 rpm). Conversions are estimated to within  $\pm 2\%$  (95% confidence)

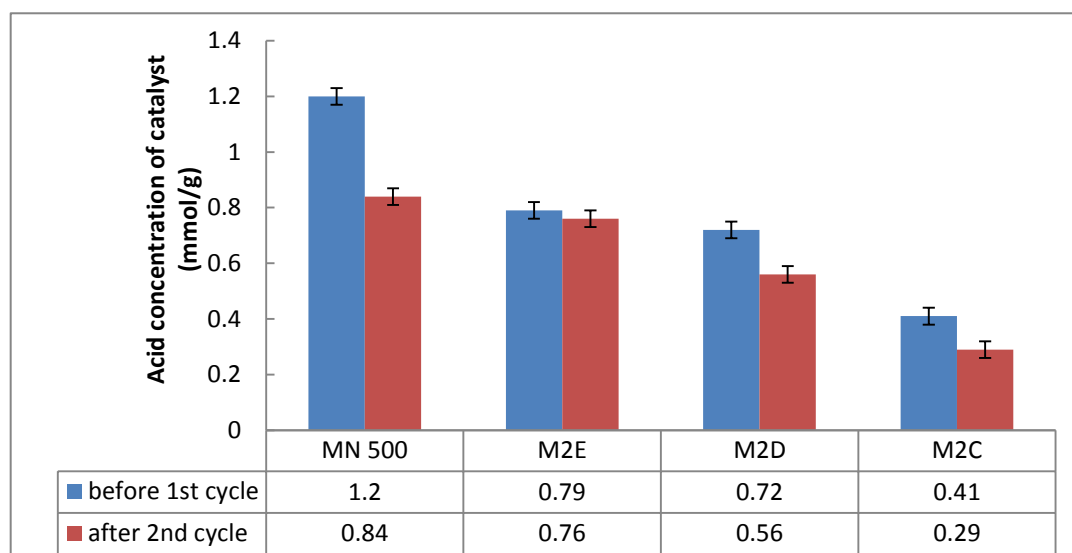


**Fig. 3.12.** Acid site concentration of each home-made catalyst before the first cycle and after the second cycle. The errors are within 0.03 mmol/g.

### 3.4. Summary of results

Four sulfonated hypercrosslinked resins were successfully synthesised by supporting sulfonic acid groups onto hypercrosslinked poly(St-DVB) MN 200 with either in-situ synthesised acetyl sulfate or concentrated sulfuric acid. The prepared samples were thoroughly washed so that leachable sulfuric acid was completely removed.

These washed samples exhibit low acid concentration, large surface area and high porosity. The home-made sample M2B along with D5081, MN 200 and Amberlyst 15 were analysed by solid-state NMR. Unfortunately, no useful information was obtained to evidence whether the methylene bridges in hypercrosslinked resins were affected by sulfonation.

The catalytic performances of the prepared catalysts were compared for the esterification of acetic acid with methanol, and were compared with those of MN 500 and Amberlyst 35. The order of activity of the hypercrosslinked catalysts is roughly in line with their acid site concentrations. Among the hypercrosslinked catalysts, M2E exhibits better reusability than M2C and M2D. This led to the conclusion that sulfonation with concentrated sulfuric acid is more effective in preventing acid site leaching.

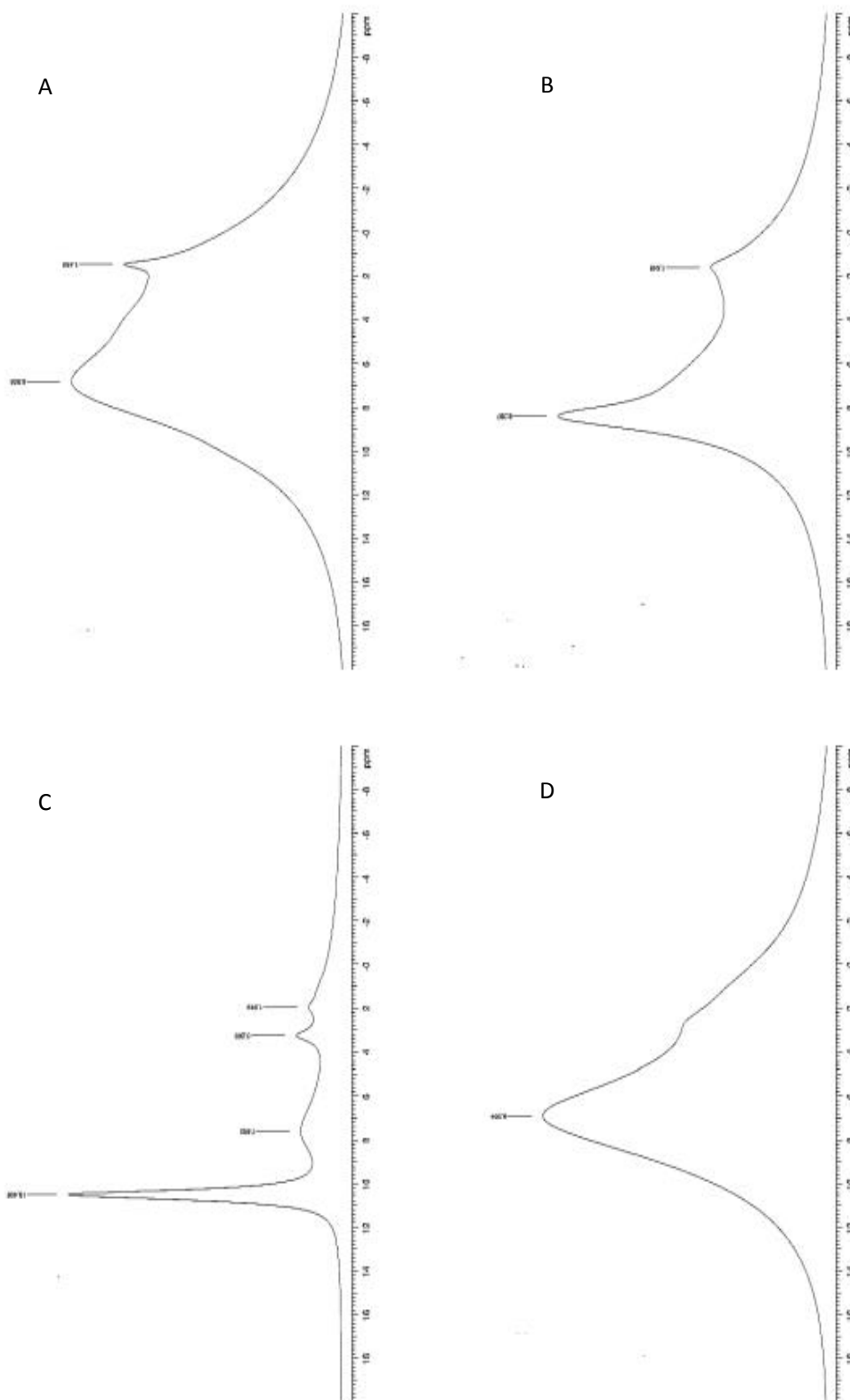


**Fig. 3.6.** Solid-state  $^1\text{H}$  NMR spectra of, MN200 (A), M2B (B), Amberlyst 15 (C) and D5081 (D).

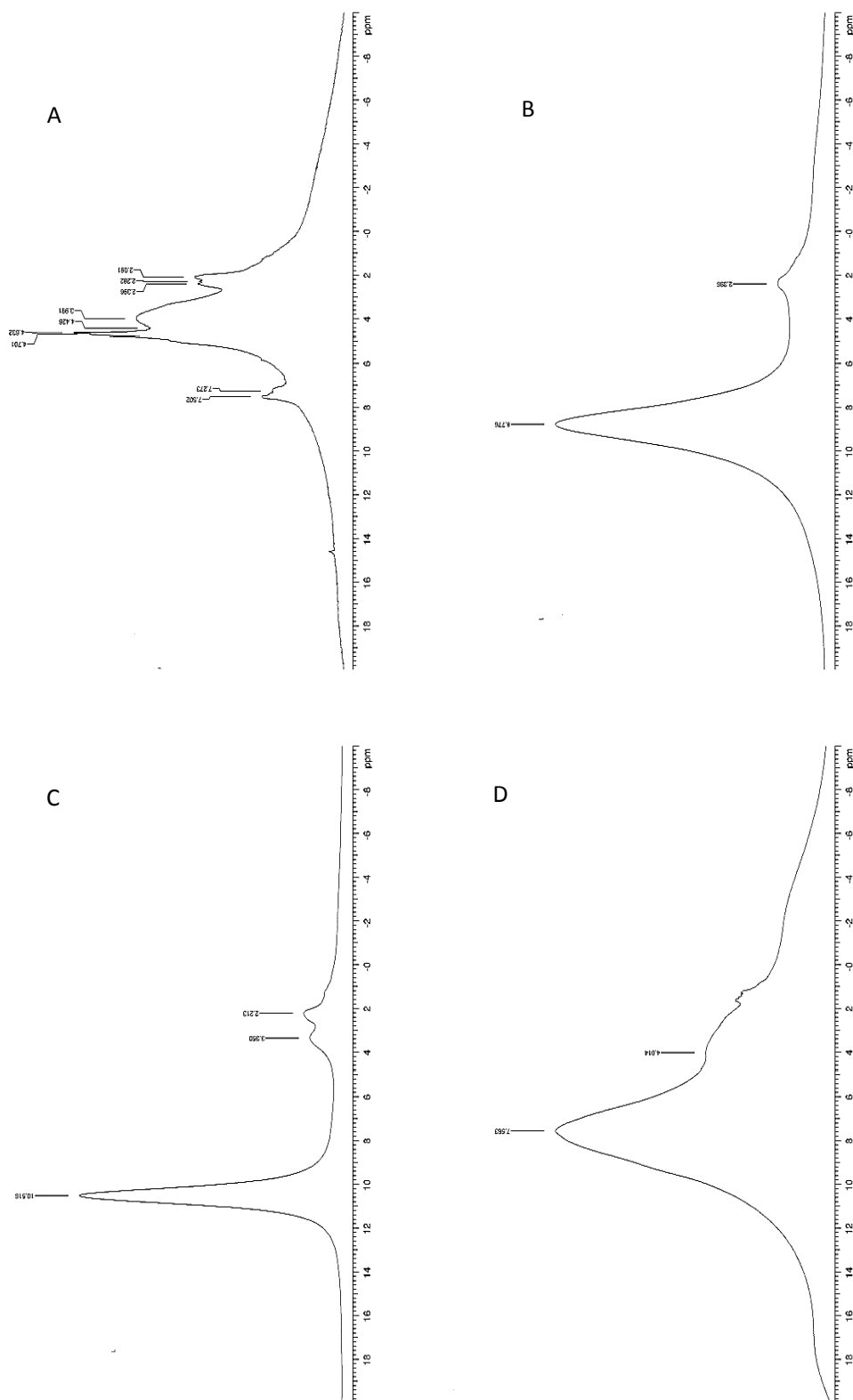


**Fig. 3.7.** Solid-state  $^1\text{H}$  NMR spectra of MN200 (A), M2B (B), Amberlyst 15 (C) and D5081 (D). The samples were pre-swollen in  $\text{CDCl}_3$ .

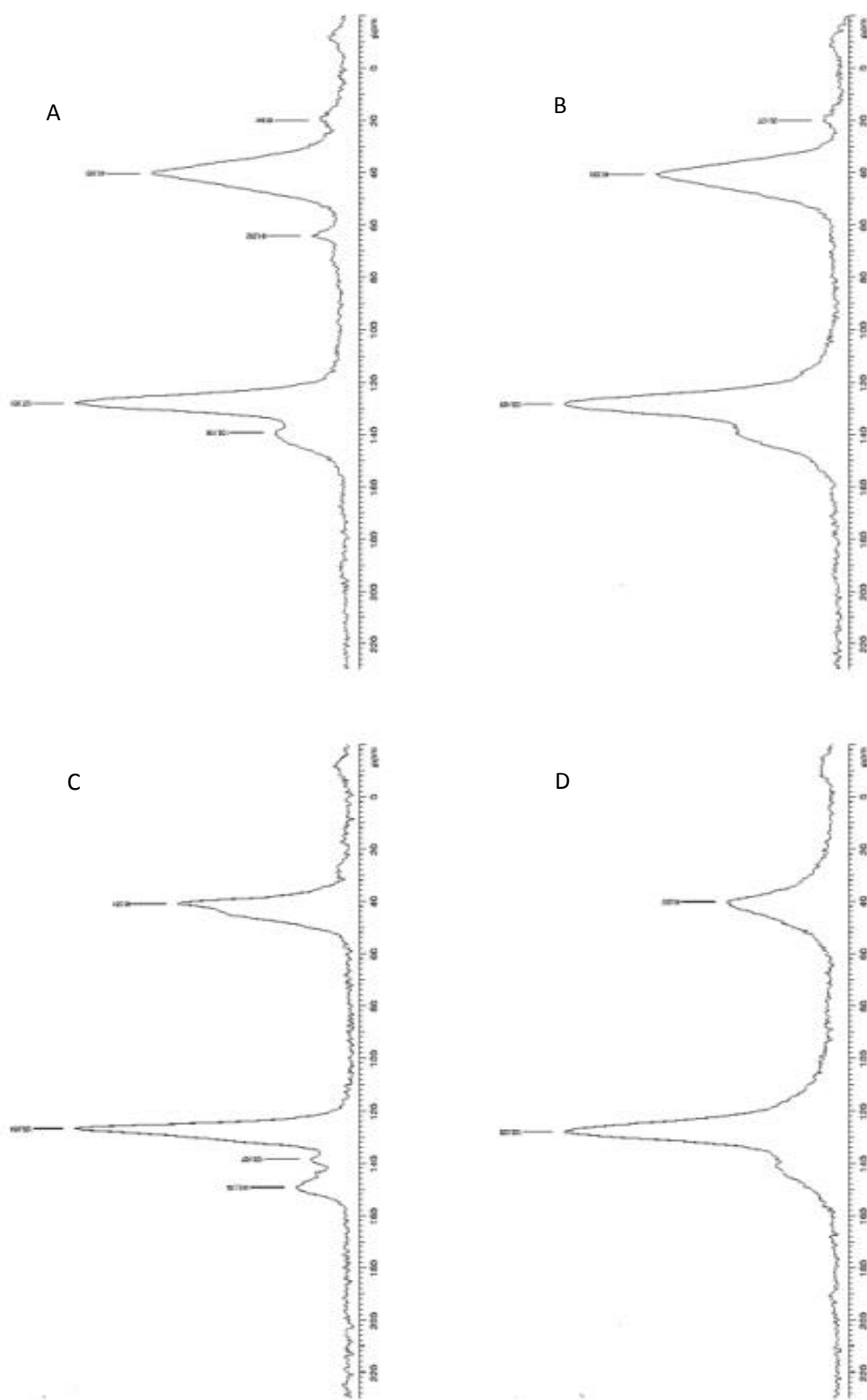


**Fig. 3.8.** Solid-state  $^{13}\text{C}$  NMR spectra of MN200 (A), M2B (B), Amberlyst 15 (C) and D5081 (D).

## References

- [1] C. A. Toro, R. Rodrigo and J. Cuellar, *React. & Funct. Polym.*, 68 (2008) 1325-1336.
- [2] M. Steenackers, S. Q. Lud, M. Niedermeier, P. Bruno, D. M. Gruen, P. Feulner, M. Stutzmann, J. A. Garrido and R. Jordan, *J. Am. Chem. Soc.*, 129 (2007) 15655-15661.
- [3] F. M. B. Coutinho, T. T. Souza and A. S. Gomes, *Europ. Polymer J.*, 40 (2004) 1525-1532.
- [4] C. Sangwichien, G. L. Aranovich and M. D. Donahue, *Colloid & Surf. A: Phys. & Eng. Asp.*, 206 (2002) 313-320
- [5] B. Li, F. Su, H. Luo, L. Liang and B. Tan, *Micro. & Mesop. Mater.* 138 (2011) 207-214.
- [6] M. P. Tsyurupa, Z. K. Blinnikova, Y. A. Davidovich, S. E. Lyubimov, A. V. Naumkin and V. A. Davankov, *React. & Funct. Polym.*, 72 (2012) 973-982.
- [7] M. P. Tsyurupa and V. A. Davankov, *React. & Funct. Polym.*, 66 (2006) 768-779.
- [8] W. W. Simons, *the Sadtler Handbook of Proton NMR Spectra*, Sadtler Research Laboratories, Heyden & Son, London, 1978.
- [9] J. M. Fraile, E. Garcia-Bordeje and L. Roldan, *J. Catal.*, 289 (2012) 73-79.
- [10] W. W. Simons, *the Sadtler Guide to Carbon-13 NMR Spectra*, Sadtler Research Laboratories, Heyden & Son, London, 1983.
- [11] R. Joseph, W. T. Ford, S. Zhang, M. P. Tsyurupa and A. V. Pastukhov, *J. Polym. Sci. Part A: Polym. Chem.*, 35 (1996) 695-701.
- [12] I. J. Dijs, H. L. F. van Ochten, A. J. M. van der Heijden, J. W. Geus and L. W. Jenneskens, *Appl. Catal. A: Gen.*, 241 (2003) 185-203.

## Chapter 4

# Kinetics of Acetic Acid Esterification Using Home-made Hypercrosslinked Poly(St-DVB) Sulfonic Acid Catalyst

### 4.1. Introduction

A series of home-made hypercrosslinked poly(St-DVB) sulfonic acids were prepared, and were thoroughly washed to remove trapped sulfuric acid before catalytic tests. Among the home-made catalysts, M2E showed good activity in the esterification of acetic acid with methanol, and no significant acid site leaching was detected on going to the second reaction cycle. Therefore, M2E was used for the kinetic modelling of esterification of acetic acid with methanol in this chapter. The pseudo-homogeneous, Eley-Rideal and Langmuir-Hinshelwood models were compared to fit the kinetic profiles of the reaction. A mechanistic pathway of the esterification reaction based on the best-fit model was proposed.

### 4.2. Experimental and results

#### 4.2.1. Elimination of diffusional resistances

In the kinetic modelling experiments, the reaction conditions were set such that a known amount of acetic acid reacts with excess methanol at 60 °C using the batch setup applied in previous chapters. External diffusion resistance was eliminated by setting the stirring speed to 600 rpm. The possible effects of internal diffusional resistance were studied through the comparison of activities of M2E in bead and in

powder forms. From **Fig. 4.1**, it can be seen that the reaction rate was hardly affected by the particle size of M2E, which suggests that the interior acid sites in M2E beads are accessible to the reactants and that the effectiveness factor for catalysis is unity. Therefore, it is reasonable to conclude that the entire catalytic process is kinetically controlled when M2E is in beads under these reaction conditions. Since the diffusional resistances (both internal and external) are absent, the kinetic modelling can be conducted with M2E in beads.

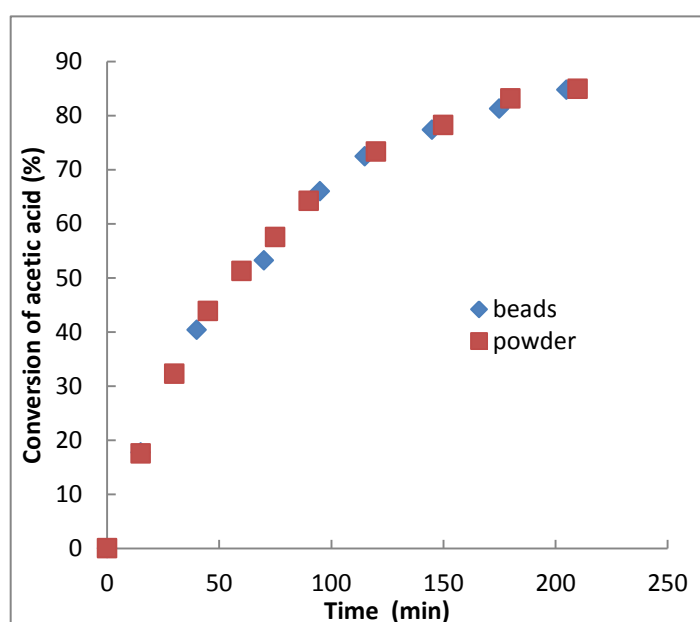


**Fig. 4.1.** Effect of particle size of M2E in acetic acid esterification with methanol (acetic acid: 4.00 g, methanol: 20.0 g, Catalyst amount: 0.200 g, temperature: 60 °C, stirring speed: 600 rpm).

#### 4.2.2. Kinetic modelling with pseudo-homogeneous model

The esterification reaction between acetic acid and methanol can be represented in the following schematic form:



As an analogue of the homogeneous acid catalysis, the sulfonated hypercrosslinked poly(St-DVB) in esterification is to be treated as a source of solvated protons. Thus, the reaction was assumed to follow second-order kinetics with first order for each reactant. Then the pseudo-homogeneous model for the reaction rate is written as

$$r = k \left( C_M C_A - \frac{C_E C_W}{K_{eq}} \right) \quad (\text{Eq. 4.2})$$

where  $C_A$ ,  $C_M$ ,  $C_W$  and  $C_E$  are the concentrations of methanol, acetic acid, water and methyl acetate respectively,  $k$  is the rate constant and  $K_{eq}$  is the reaction equilibrium constant. At the initial stage of the reaction, the term of reverse reaction only has a minimal effect; hence the rate equation is simplified to

$$r_0 = k C_M C_A = C_{A,0} \frac{dX_A}{dt} \quad (\text{Eq. 4.3})$$

Where  $r_0$  is the initial reaction rate,  $C_{A,0}$  is the initial concentration of acetic acid,  $C_M$  and  $C_A$  are the concentrations of methanol and acetic acid respectively at a certain time,  $X_A$  is the conversion ratio of acetic acid, and  $t$  is the reaction time. **Table 4.1** summaries the initial reaction rates with according initial concentrations of methanol and acetic acid. The initial reactions rates were experimentally obtained from the conversion ratios of acetic acid in the first 9 minutes of the reaction which was determined by acid/base titration of withdrawn sample from the reaction mixture. The experimental procedures were the same as those stated for conversions of carboxylic acids in previous chapters. The reaction temperature was set at 60 °C and the stirring speed was 600 rpm. THF was introduced as the solvent

to fix the volume of reaction mixture at 29.0 ml. The effect of THF on the initial reaction is minor given the large quantity of reactants used [1].

**Table 4.1.** Initial reaction rate data for the esterification of acetic acid with methanol at 60 °C and stirring speed of 600 rpm ( $C_{M,0}$  and  $C_{A,0}$  are the initial concentrations of methanol and acetic acid added to the reaction, and  $r_0$  is the initial reaction rate,  $n$  is the molar ratio of methanol to acetic acid)

$C_{M,0}$ (M)	$C_{A,0}$ (M)	$n$	$r_0$ (M/min) <sup>1</sup>
4.305	2.297	1.874	0.00924
8.610	2.297	3.748	0.0166
12.91	2.297	5.620	0.0246
17.22	2.297	7.497	0.0291
21.52	2.297	9.375	0.0339
17.22	1.148	15.00	0.0153
17.22	3.445	4.999	0.0430
17.22	4.594	3.748	0.0543

1. The error is 5%

To determine the rate constant, the calculated conversion ratios of acetic acid ( $X_A$ ) can be substituted to the following equation which is rearranged from **Eq. 4.3**:

$$\frac{dX_A}{dt} = kC_{A,0}(n - X_A)(1 - X_A), \quad (\text{Eq. 4.4})$$

which is then integrated to give:

$$\ln\left(\frac{n-1+X_A}{1-X_A}\right) = kC_{A,0}(n-1)t + \text{constant}, \quad (\text{Eq. 4.5})$$

where  $n$  is the molar ratio of methanol to acetic acid.

With known time ( $t$ ) and molar ratio ( $n$ ), the term  $C_{A,0}(n-1)t$  is also known. If this esterification reaction catalysed by M2E would follow the second-order kinetics, the rate constant,  $k$ , can be determined from the gradient of the linear plot of  $\ln\left(\frac{n-1+X_A}{1-X_A}\right)$

against  $C_{A,0}(n-1)t$ . The data in **Table 4.1** were used for this plot. However, the plot shows a nonlinear relationship between these two terms with the correlation coefficient of 0.8031 (**Fig. 4.3**), hence it is not reliable to say this gradient represents the rate constant. In other words, this result revealed that the pseudo-homogeneous model is not fit for this reaction.

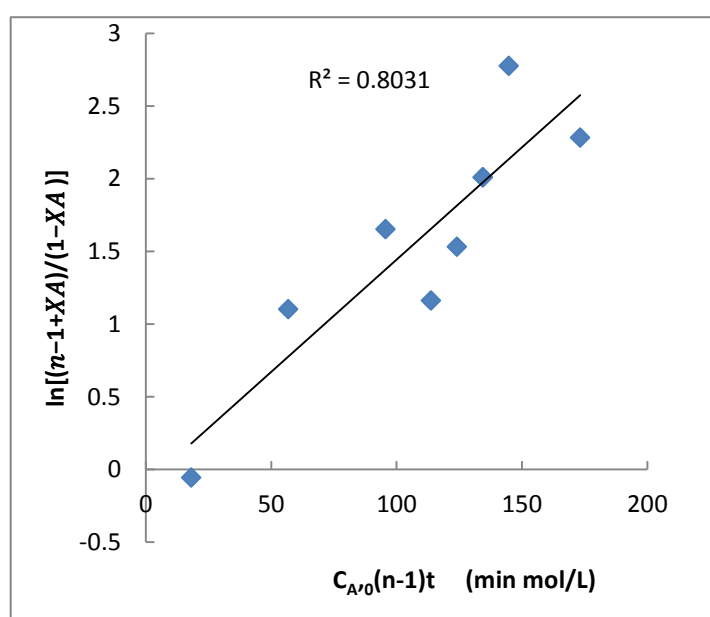


**Fig. 4.3.** The plot of  $\ln\left(\frac{n-1+X_A}{1-X_A}\right)$  against  $C_{A,0}(n-1)t$  to determine the rate constant of esterification of acetic acid with methanol by applying pseudo-homogeneous model.

Alternatively, the fitness of pseudo-homogenous model for the esterification reaction catalysed by M2E can be tested using power law approximation. This was done by determining the kinetic order of each reactant separately according to the following rate equation:

$$\ln r_0 = \ln k' + \alpha \ln C_0 \quad (\text{Eq. 4.6})$$

where  $r_0$  is the initial reaction rate,  $k'$  is a lump rate constant,  $\alpha$  is kinetic order of each reactant and  $C_0$  is the initial concentration of each reactant. By the linear plot of  $\ln r_0$  against  $\ln C_0$ , the apparent kinetic orders were determined to be 0.92 for acetic acid and 0.82 for methanol, with the correlation coefficients of 0.99-1.00 (**Fig. 4.2**). Both of the kinetic orders for acetic acid and methanol were found to be lower than 1, which, again, indicated the pseudo-homogeneous model was not the best choice for the esterification reaction. Based on these findings, the Eley-Rideal and Langmuir-Hinshelwood models were considered in the next sections.

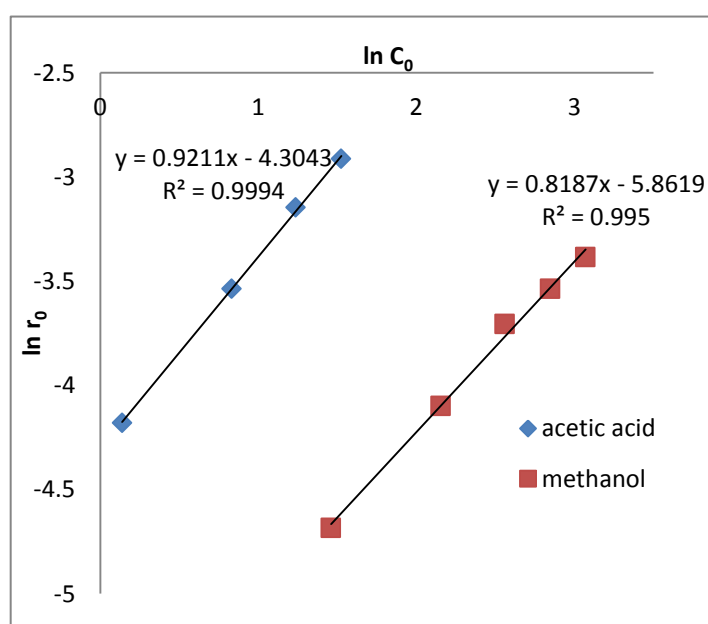


**Fig. 4.2.** Kinetic order determination for methanol and acetic acid in the esterification catalysed by M2E.  $C_0$  is the initial concentration of each reactant.  $r_0$  is the initial reaction rate.

#### 4.2.3. Kinetic modelling with the Eley-Rideal model

The Eley-Rideal model assumes that the rate-limiting step is the surface reaction which takes place between the adsorbed reactant and the other non-adsorbed

reactant from the bulk liquid [2]. The Eley-Rideal model was developed to interpret kinetics of reactions which involve gas being adsorbed onto solid surface, and have also been applied for the liquid phase reactions over solid catalysts [3-6]. In the solid acid catalysed esterification, the mechanism is shown as below [1]:



where M represents methanol, S is a vacant acid site on the catalyst surface, A is acetic acid, MA is methyl acetate, W is water and asterisks indicate adsorbed species. The affinity of sulfonated resin catalyst for water, alcohol and carboxylic acid is much stronger than that for the ester [7]. Hence the adsorption term for methyl ester is neglected in the E-R model. The rate expression for the E-R model then is

$$r = -\frac{dC_A}{dt} = \frac{k}{1 + K_A C_A + K_M C_M + K_W C_W} \times \left( C_A C_M - \frac{C_{MA} C_W}{K_{eq}} \right), \quad (\text{Eq. 4.7})$$

where  $C_A$ ,  $C_M$ ,  $C_W$  and  $C_{MA}$  are the concentration of methanol, acetic acid, water and methyl acetate respectively,  $k$  is the rate constant which takes account of the amount of the catalyst.  $K_A$ ,  $K_M$  and  $K_W$  are the adsorption equilibrium constants for acetic acid, methanol and water:

$$K_M = \frac{k_1}{k_{-1}}, \quad (\text{Eq. 4.8})$$

$$K_A = \frac{k_2}{k_{-2}}, \quad (\text{Eq. 4.9})$$

$$K_W = \frac{k_4}{k_{-4}}. \quad (\text{Eq. 4.10})$$

The reverse reaction at the initial stage of the reaction is negligible so the term of adsorption of water is omitted to give the initial rate:

$$r_0 = \frac{kC_A C_M}{1 + K_A C_A + K_M C_M}. \quad (\text{Eq. 4.11})$$

Taking the reciprocal of this equation and fixing  $C_A$  constantly, a plot of  $1/r_0$  versus  $1/C_{M,0}$  could yield a straight line by varying  $C_{M,0}$ . The ratio of the gradient against intercept is equal to  $\frac{1+K_A C_{A,0}}{K_M}$  in **Eq. 4.12**. Accordingly, the value of  $\frac{1+K_M C_{M,0}}{K_A}$  could be determined from the linear plot of  $1/r_0$  versus  $1/C_{A,0}$  in **Eq. 4.13**. The plots are shown in **Figs. 4.4** and **4.5**.

$$\frac{1}{r_0} = \frac{K_M}{kC_{A,0}} + \frac{1 + K_A C_{A,0}}{kC_{A,0}} \times \frac{1}{C_{M,0}}, \quad (\text{Eq. 4.12})$$

$$\frac{1}{r_0} = \frac{K_A}{kC_{M,0}} + \frac{1 + K_M C_{M,0}}{kC_{M,0}} \times \frac{1}{C_{A,0}}. \quad (\text{Eq. 4.13})$$

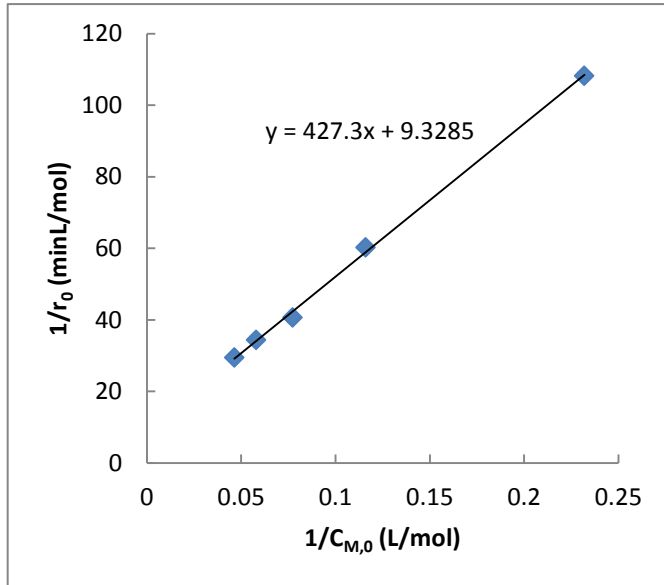


**Fig. 4.4.** The plot of  $1/r_0$  versus  $1/C_{M,0}$  for determination of adsorption equilibrium constants.

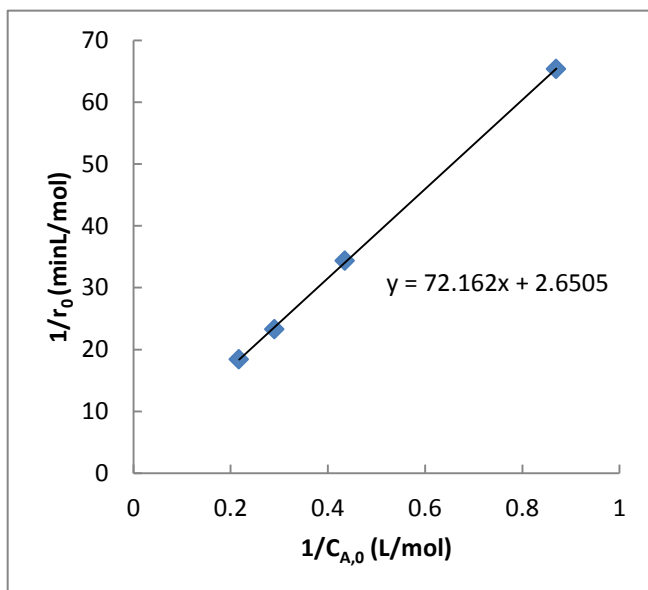


**Fig. 4.5.** The plot of  $1/r_0$  versus  $1/C_{A,0}$  for determination of adsorption equilibrium constants.

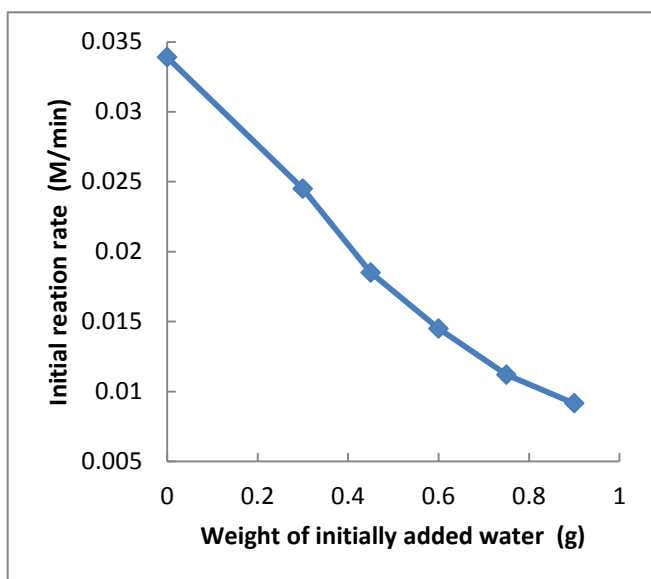


**Fig. 4.6.** The effect of water amount in the reaction mixture on the initial reaction rate.

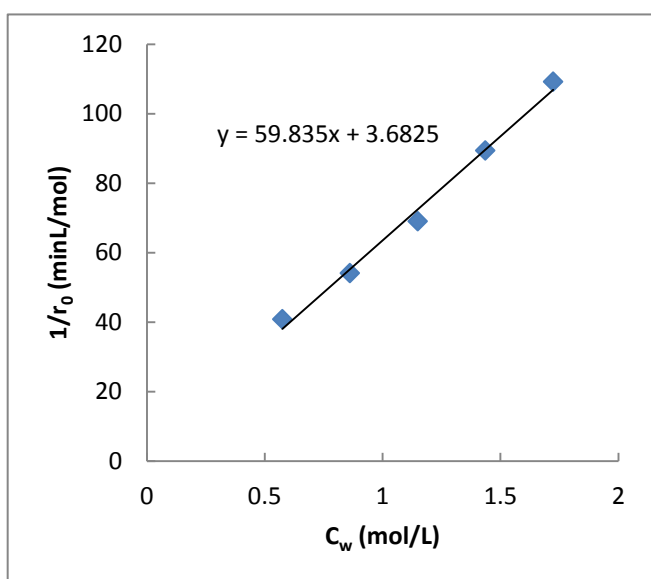


**Fig. 4.7.** The plot of  $1/r_0$  versus  $C_w$  for determination of the adsorption equilibrium constant of water.

The effect of water on activity of the catalyst was studied by varying the amount of initially added water. The concentrations of acetic acid and methanol were fixed at 17.22 M and 2.297 M with THF to maintain the total volume at 29.0 ml. As shown in **Fig. 4.6**, water can seriously decelerate the rate of the reaction, so the adsorption term of water should be included in the kinetic expression (**Eq. 4.14**). From the

reciprocal form of this kinetic expression (**Eq. 4.15**), a plot of  $1/r_0$  versus  $C_{w,0}$  could yield a straight line, and  $K_w$  can be calculated from the intercept with the determined values of  $K_M$ ,  $K_A$  and  $k$ . The plot is shown in **Fig. 4.7**. The reaction equilibrium constant,  $K_{eq}$ , was calculated from the product of the concentrations of both reactants and products and was found to be 10.9 under these reaction conditions.

$$r_0 = \frac{kC_A C_M}{1 + K_A C_A + K_M C_M + K_W C_w}, \quad (\text{Eq. 4.14})$$

$$\frac{1}{r_0} = \frac{1 + K_A C_{A,0} + K_M C_{M,0}}{kC_{A,0} C_{M,0}} + \frac{K_W}{kC_{A,0} C_{M,0}} \times C_{w,0}. \quad (\text{Eq. 4.15})$$

**Table 4.2.** summarises the values of  $K_M$ ,  $K_A$ ,  $k_w$ ,  $k$  and  $K_{eq}$  (at 60 °C) which could be substituted into the rate equation of **Eq. 4.7** to obtain the following expression in terms of acetic acid conversion ratio, and this is the specified Eley-Rideal model for the esterification of acetic acid with methanol over M2E catalyst:

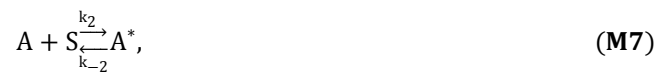
$$\frac{dX_A}{dt} = \frac{0.00269C_{A,0}}{1 + C_{A,0}[0.0536(n - X_A) + 0.0267(1 - X_A) + 5.49X_A]} \times \left[ (n - X_A)(1 - X_A) - \frac{X_A^2}{10.9} \right]. \quad (\text{Eq. 4.16})$$

**Table 4.2.** The parameters for E-R and L-H models in fitting the experimental data

Model	k	$K_M$	$K_A$	$K_w$	$K_{eq}$ (60 °C)
E-R	0.00269	0.0536	0.0267	5.49	10.9
L-H	0.00110	0.0102	0.0177	0.00160	10.9

#### 4.2.4. Kinetic modelling with the Langmuir-Hinshelwood model

The Langmuir-Hinshelwood model was also applied for the solid acid catalysed liquid phase esterifications in which the rate-limiting step was assume to be the surface reaction between adsorbed acetic acid and adsorbed methanol [8]:



The rate expression for the L-H model is presented in **Eq. 4.17** by taking account of adsorption terms of water, alcohol and carboxylic acid, and the reverse reaction:

$$r = -\frac{dC_A}{dt} = \frac{k}{(1 + K_A C_A + K_M C_M + K_W C_W)^2} \times \left( C_A C_M - \frac{C_{MA} C_W}{K_{eq}} \right). \quad (\text{Eq. 4.17})$$

$$r_0 = \frac{k C_A C_M}{(1 + K_A C_A + K_M C_M)^2}, \quad (\text{Eq. 4.18})$$

$$r_0 = \frac{k C_A C_M}{(1 + K_A C_A + K_M C_M + K_W C_W)^2}. \quad (\text{Eq. 4.19})$$

The initial rate equations expressed as **Eqs. 4.18** and **4.19**. The latter equation takes account of the adsorption of the catalyst on water. **Eqs. 4.20** and **4.21** were rearranged from the root squared forms of the reciprocal of **Eq. 4.18** and could be generalised to the functions of  $y=a/x+bx$  which were plotted with varied  $\sqrt{C_{M,0}}$  or

$\sqrt{C_{A,0}}$  in each rearranged equation to calculate the values of a and b and the results are shown in **Table 4.3** with R-square value of 0.998 and 1.00. The data used for plotting and calculation were from **Table 4.1**. With the values of a and b,  $K_M$ ,  $K_A$  and k were calculated. **Eq. 4.22** was derived from the root squared form of the reciprocal of the Langmuir-Hinshelwood model expression of **Eq.4.19** and  $K_w$  was subsequently determined from the linear plot of  $\sqrt{\frac{1}{r_0}}$  against  $C_{w,0}$  (**Fig. 4.8**).  $K_{eq}$  is also 10.9 in this case.

$$\sqrt{\frac{1}{r_0}} = \frac{1 + K_A C_{A,0}}{\sqrt{k C_{A,0}}} \times \frac{1}{\sqrt{C_{M,0}}} + \frac{K_M}{\sqrt{k C_{A,0}}} \times \sqrt{C_{M,0}}, \quad (\text{Eq. 4.20})$$

$$\sqrt{\frac{1}{r_0}} = \frac{1 + K_M C_{M,0}}{\sqrt{k C_{M,0}}} \times \frac{1}{\sqrt{C_{A,0}}} + \frac{K_A}{\sqrt{k C_{M,0}}} \times \sqrt{C_{A,0}}, \quad (\text{Eq. 4.21})$$

$$\sqrt{\frac{1}{r_0}} = \frac{1 + K_A C_{A,0} + K_M C_{M,0}}{\sqrt{k C_{A,0} C_{M,0}}} + \frac{K_w}{\sqrt{k C_{A,0} C_{M,0}}} \times C_{w,0}. \quad (\text{Eq. 4.22})$$

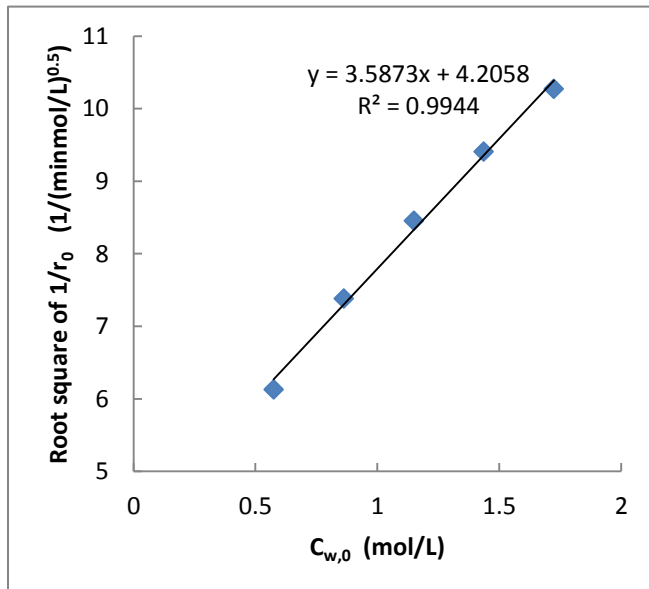


**Fig. 4.8.** Determination of adsorption equilibrium constant of water ( $K_w$ ) in L-H model

The values of  $K_M$ ,  $K_A$ ,  $k_w$ ,  $k$  and  $K_{eq}$  (at 60 °C) are also summarised in **Table 4.2**.

Applying these parameters, the rate equation based on the Langmuir-Hinshelwood model was derived in terms of acetic acid conversion ratio for the esterification reaction:

$$\frac{dX_A}{dt} = \frac{0.00110C_{A,0}}{\left(1 + C_{A,0}\left[0.0102(n - X_A) + 0.0177(1 - X_A) + 0.00160X_A\right]\right)^2} \times \left[ (n - X_A)(1 - X_A) - \frac{X_A^2}{10.9} \right]. \quad (\text{Eq. 4.23})$$

**Table 4.3.** The values of a and b determined for  $y=a/x+bx$  which represents **Eqs. 4.20** and **4.21**

	<b>a</b>	<b>b</b>	<b>R-square</b>
<b>Eq. 20</b>	20.77	0.2016	0.998
<b>Eq. 21</b>	8.508	0.1463	1.00

#### 4.2.5. Model verification

In this section, the derived E-R and L-H models were tested whether they could best fit the esterification of acetic acid with methanol over M2E catalyst under the given reaction conditions. To calculate the integral of acetic conversion ( $X_A$ ) upon specific reaction time ( $t$ ), the differentiated rate equations of the E-R and the L-H models (**Eq. 4.16** and **4.23**) is rearranged to give the integrated conversion of acetic acid which is defined as:

$$X_A = \int_0^t \frac{dX_A}{dt} = \int_0^t f(X_A). \quad (\text{Eq. 4.24})$$

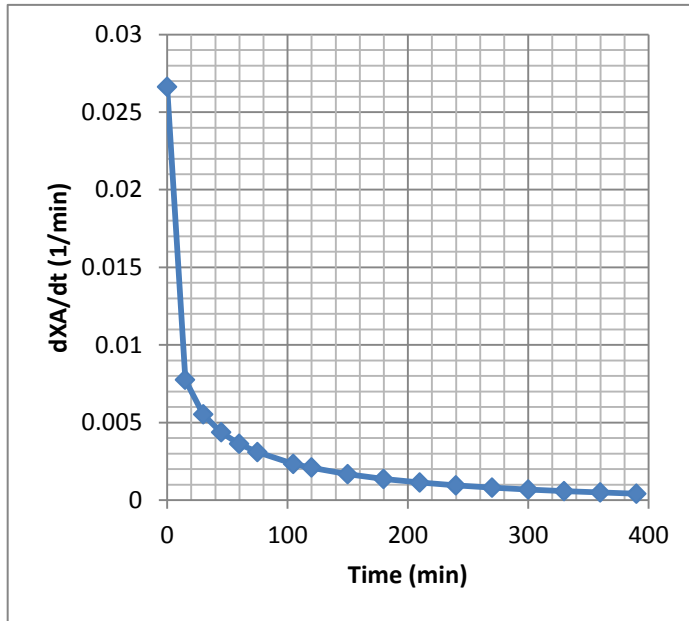


**Fig 4.9.** The plot of  $f(X_A)$  against time ( $t$ ) to determine the conversion of acetic acid at specific time.

Then integrated  $f(X_A)$  is the sum of the area enclosed by the entire plot and the interval of  $[0, t]$ . When the interval  $[0, t]$  is subdivided into  $i$  subintervals ( $i=2, 3, 4, \dots$ ) which are small enough, the shape enclosed by the curve and a subinterval can be regarded as a trapezium [8]. Therefore the sum of the areas of the trapezia (**Fig. 4.9**) is equal to the acetic acid conversion ratio which is calculated by

$$X_{A,t_i}^{\text{output}} = \frac{1}{2} (t_i - t_{i-1}) [f(X_{A,t_i}^{\text{input}}) + f(X_{A,t_{i-1}}^{\text{input}})] + X_{A,t_{i-1}}^{\text{output}} \quad (\text{Eq. 4.25})$$

where *input* denotes the variable of  $X_A$  in the rate expression of **Eq. 4.16** and **4.23**, and *output* denotes the dependent variable of  $X_A$  which is calculated by an input value.

The determination of the true value of  $X_A$  was performed by adjusting  $X_{A,t_n}^{\text{input}}$  until the minimisation of the sum of residual squares (SRS) is satisfied [9] between

conversion ratio inputs ( $X_{A,t_n}^{input}$ ) and the conversion ratio output ( $X_{A,t_n}^{output}$ ). In this case, the criterion is SRS being minimised to  $10^{-10}$ .

$$SRS = \sum_{i=1}^n (X_{A,t_i}^{input} - X_{A,t_i}^{output})^2 \quad (\text{Eq. 4.26})$$

The  $X_{A,t_1}$  denotes the conversion ratio of acetic acid at the very beginning of reaction:

$$X_{A,t_1}^{input} = X_{A,t_1}^{output} = 0 \quad (\text{Eq. 4.27})$$

In the integration for  $X_A$ , the effect of sample withdrawing was taken into account by introducing a correction of total volume ( $V_{tot}$ ) of the liquid mixture corresponding to the sample volume ( $v$ ) of 0.7 ml. Therefore,  $C_{A,0}$  in the kinetic equations of the E-R model and the L-H model were replaced by  $C_A$  to verify the model application:

$$C_A = C_{A,0} \frac{V_{tot}}{V_{tot} - (i-1)v} \quad (i = 1, 2, 3 \dots). \quad (\text{Eq. 4.28})$$

The mean relative deviations (MRDs) were calculated between the experimental and calculated conversion ratios from each model equation to judge the fitness of the models to the experimental results [9]:

$$MRD = \frac{1}{n} \sum_{i=1}^n \sqrt{\left(1 - \frac{X_{A,t_i}^{output}}{X_{A,t_i}^{expt}}\right)^2}. \quad (\text{Eq. 4.29})$$

$X^{expt}$  is the calculated conversion ratio of acetic acid.

Two sets of experimental results with methanol to acetic acid molar ratio of 9.375 and 5 were used for the comparison for both E-R model and L-H model in **Fig. 4.10-4.12**. By controlling SRS lower than  $10^{-10}$ , it was found that the mathematical derivation of the E-R model successfully predicted the reaction profiles of the esterification of acetic acid in the presence of excess methanol over M2E catalysis, judged from prediction plots and the values of MRD (**Table 4.4**).

**Table 4.4.** Statistic comparison of different kinetic models in fitting the experimental results

Model	n	SRS	MRD
E-R	9.375	$4.81 \times 10^{-11}$	0.0341
	5	$3.46 \times 10^{-11}$	0.0412
L-H	9.375	$1.71 \times 10^{-11}$	0.142
	5	$1.66 \times 10^{-11}$	0.230

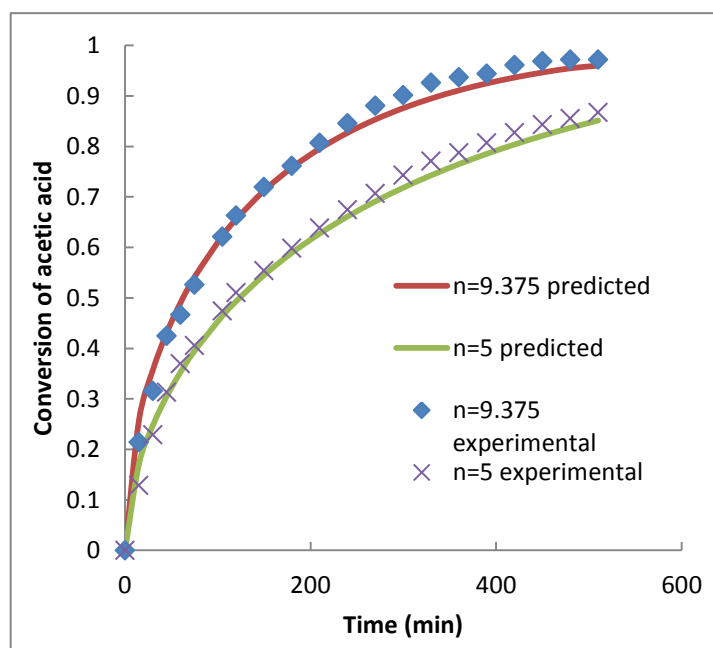


**Fig. 4.10.** Comparison between experimental data and values predicted by E-R model (n is the methanol to acetic acid molar ratio, n= 9.375 was from 4.00 g acetic acid and 20.0 g methanol, n=5 was from 6.00 g acetic acid and 16.0 g methanol, catalyst amount: 0.200 g, temperature: 60 °C, stirring speed: 600 rpm).

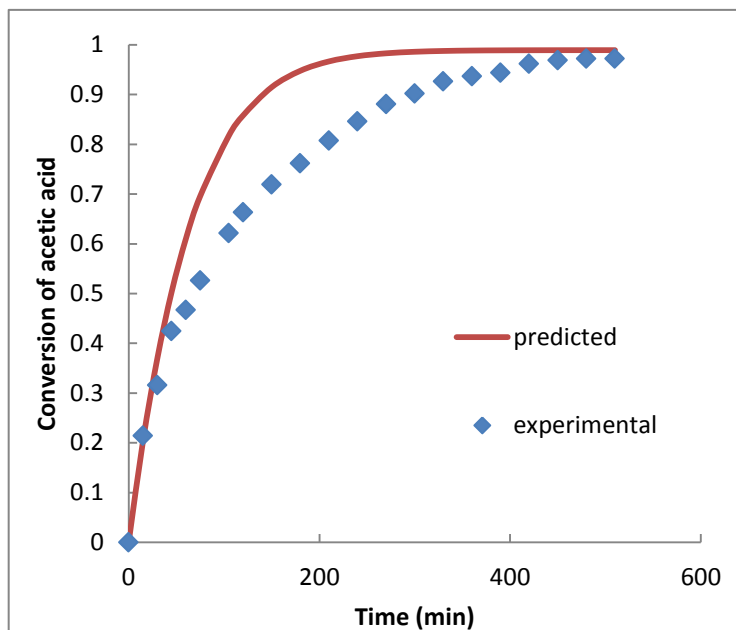


**Fig 4.11.** Comparison between experimental data and prediction of L-H model when methanol to acetic acid molar ratio ( $n$ ) is 9.375 (acetic acid: 4.00 g, methanol: 20.0 g, temperature: 60 °C, catalyst amount: 0.200 g, stirring speed: 600 rpm).

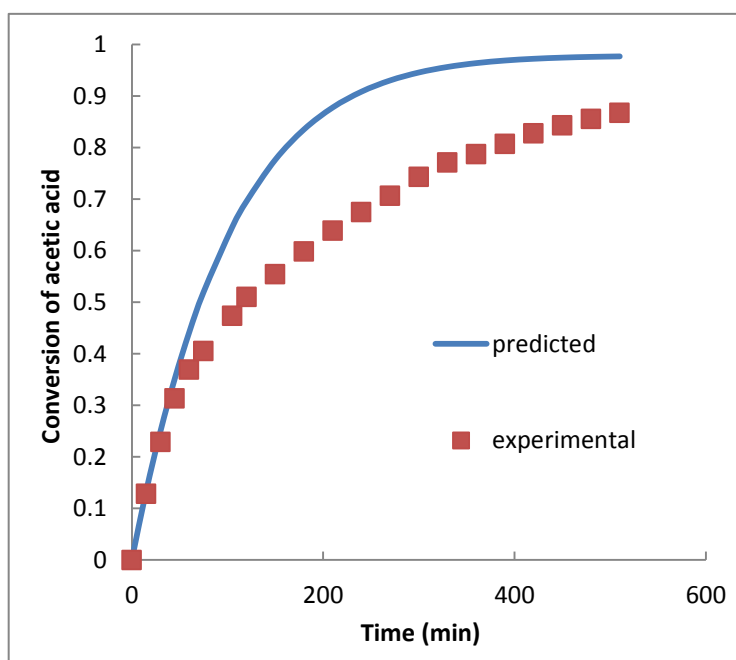


**Fig 4.12.** Comparison between experimental data and prediction of L-H model when methanol to acetic acid molar ratio ( $n$ ) is 5 (acetic acid: 6.00 g, methanol: 16.0 g, temperature: 60 °C, catalyst amount: 0.200 g, stirring speed: 600 rpm).

### 4.3. Discussion

The esterification reaction was confirmed to be absent of diffusion limitations, which enabled reliable interpretation of the intrinsic reaction kinetics. The experimental and modelling results supported that the Eley-Rideal model best fits the esterification of acetic acid with methanol catalysed by M2E where adsorbed and protonated acetic acid molecules react with non-adsorbed methanol molecules (**Fig. 4.13**). This nucleophilic attack yields a tetrahedral intermediate which is converted to another form of tetrahedral intermediate by proton transfer, followed by the water molecule leaving the backbone of the intermediate. Finally, the catalyst is regenerated and methyl acetate is produced when the hydrogen-oxygen bond breaks between the sulfonic acid group and the protonated ester.

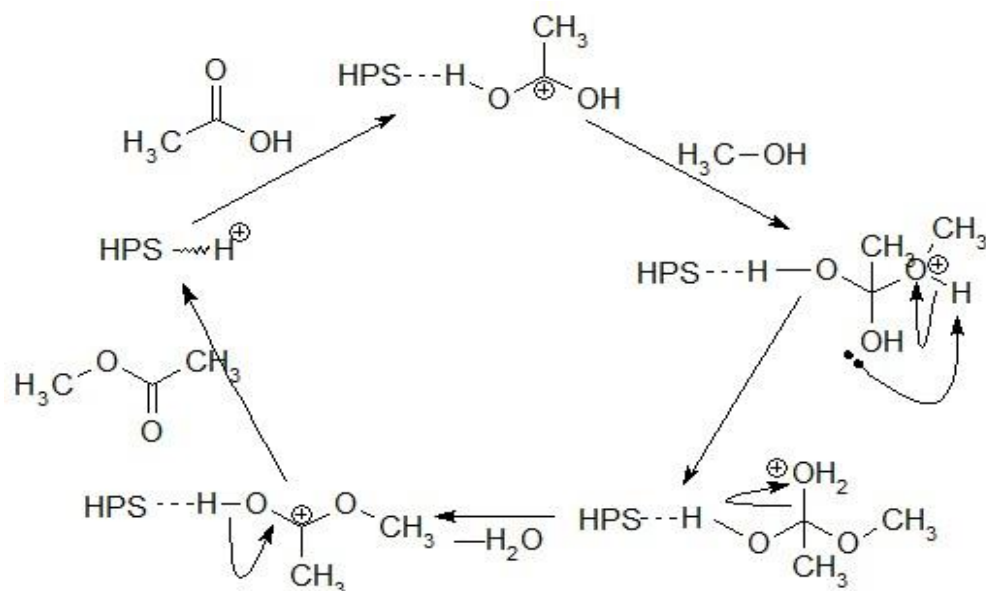


**Fig. 4.13.** Mechanistic pathway of acetic acid esterification with methanol catalysed by hypercrosslinked poly(St-DVB) sulfonic acid M2E which is replaced with HPS-H in the figure.

The kinetics of the reaction are strongly affected by competitive adsorption between the reactants and products as shown in **Fig. 4.14**. (a) Acetic acid molecules compete to adsorb on the acid sites with methanol. (b) In the reaction step, acetic acid accepts a proton from the acid site of M2E and is attacked by methanol molecule to give a protonated ester and water. (c) The proton on the ester molecule is lost and is gained by methanol molecule. (d) The protonated methanol desorbs and the acid site is occupied by water. Being continuously produced, water molecules are retained on the acid sites. As seen from **Table 4.3**, the magnitude of adsorption strength follows the order of water  $\gg$  methanol  $>$  acetic acid in E-R model and the ratio of the adsorption constants of acetic acid: methanol: water is 0.0049:0.0098:1. This means the overall kinetics overwhelmingly favours the forward direction of adsorption of water (Step d); as a sequence, the surface reaction (Step b) is inevitably inhibited.

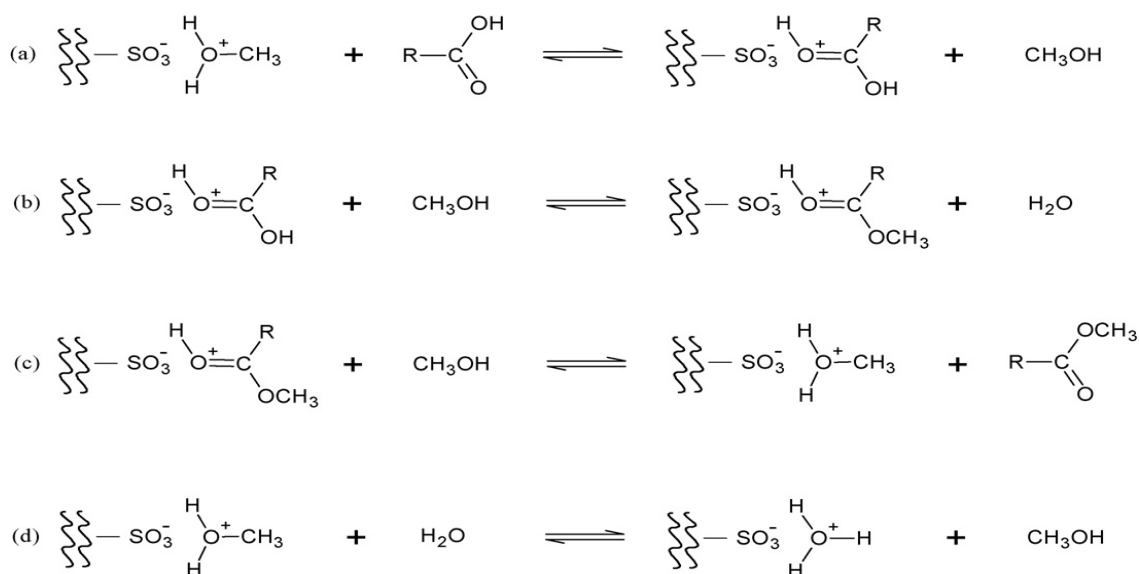


**Fig. 4.14.** Competitive adsorptions of the reactants and products on the acid sites of hypercrosslinked poly(St-DVB) sulfonic acid catalyst M2E in the esterification of carboxylic acid with methanol.

#### **4.4. Summary of results**

This chapter focused on the kinetics of acetic acid esterification with methanol over hypercrosslinked poly(St-DVB) sulfonic acid M2E catalysis. The kinetic profiles were mathematically derived from integrated expression of acetic acid conversion, from which it was found that the Eley-Rideal model with adjusted parameters best fits the experimental data. Because of preferable adsorption on the acid sites of the catalyst, water severely inhibits the catalyst activity.

## References

- [1] Y. Liu, E. Letero and J. G. Goodwin Jr, *J. Catal.*, 242 (2006) 278-286.
- [2] G. Barnes and I. Gentle, *Interfacial Science: an Introduction*, Oxford University Press, Oxford, 2005.
- [3] A. Corma, V. Martinez-Soria and E. Schnoefeld, *J. Catal.*, 192 (2000) 163-173.
- [4] W-T, L and C-S. Tan, *Ind. Eng. Chem. Res.*, 40 (2001) 3281-3286.
- [5] T. F. Dossin, M-F. Teyniers and G. B. Martin, *Appl. Catal. B: Envir.*, 62 (2006) 35-45.
- [6] V. Belliere, C. Lorentz, C. Geantet, Y. Yoshimura, D. Laurenti and M. Vrinat, *Appl. Catal. B: Envir.*, 64 (2006) 254-261.
- [7] T. A. Nijhuis, A. E. W. Beers, F. Kapteijn and J. A. Moulijn, *Chem. Eng. Sci.*, 57 (2002) 1627-1632.
- [8] K. D. Joshi, *Calculus for Scientists and Engineers: An Analytical Approach*, Alpha Science, Pangbourne, 2002.
- [9] S. Miao and B. H. Shanks, *J. Catal.*, 279 (2011) 136-143.

## Chapter 5

# Home-made Hypercrosslinked Poly(St-DVB) Sulfonic Acid Catalysts for the Esterification of Free Fatty Acids in Biodiesel Synthesis

### 4.1. Introduction

The esterification of free fatty acids (FFAs) in biodiesel synthesis has been intensively studied on solid acid catalysis. However, the use of hypercrosslinked polymer supported sulfonic acids as the catalysts has been rarely investigated. In this chapter, the home-made hypercrosslinked poly(St-DVB) sulfonic acids were evaluated in the esterification of acidic oil for biodiesel synthesis. Firstly, the activity and reusability of home-made M2D and M2E were compared in pure oleic acid esterification with methanol. Secondly, M2E which showed good activity and reusability was evaluated for catalysing the esterification of oleic acid blended with rapeseed oil along with the comparison of catalytic performance of the three generations of poly(St-DVB) supported sulfonic acids (get-type C100X4, macroporous Amberlyst 35 and hypercrosslinked M2E). Later, the catalyst with the highest conversion of the FFAs in the acidic oil was chosen to evaluate the effect of reaction parameters and to optimise the reaction conditions by the use of Analysis of Variance (ANOVA). Finally, the reusability of the home-made hypercrosslinked catalyst in esterification of oil-blended oleic acid was studied.

## 5.2. Experimental method and data handling

### 5.2.1. Materials

M2D and M2E are home-made hypercrosslinked poly(St-DVB) sulfonic acids based on MacroNet 200 (Purolite Int.), Amberlyst 35 was provided by Rohm and Hass. The gel-type C100X4 resin was supplied by Purolite Int. C100X4 is sulfonated polystyrene that is cross-linked with 4% w/w of DVB. The BET surface area is  $<0.1 \text{ m}^2/\text{g}$ , and total cation exchange capacity is  $5.10 \pm 0.02 \text{ mmol/g}$  [1]. Rapeseed oil comprises 98.1% w/w triglycerides with 0.6% w/w FFAs [2]. Cooked rapeseed oil contains a high content of FFAs, most of which is oleic acid. Therefore the fresh rapeseed oil blended with oleic acid (32 wt. %) was used to simulate waste cooking oil (WCO) for the FFA esterification with methanol in biodiesel synthesis. The rapeseed oil was purchased from a local supermarket. Methanol (99.5+ %) and oleic acid (99.7+ %) were provided by Fisher Scientific, UK.

### 5.2.2. Experimental design

The esterification experiments were carried out in a laboratory-scale batch reactor using the same method as was stated in the previous chapters. For the pure oleic esterification, the experimental conditions was set to be the same as for the esterification procedure in Chapter 2 with the temperature lowered to  $60 \text{ }^\circ\text{C}$  to reduce methanol vaporisation. For the oil-blended esterification, the standard conditions were that 5.00 g methanol was reacted with 16.0 g blended rapeseed oil (the oil to oleic acid mass ratio is 11:5) over 0.20 g pre-dried M2E at  $60 \text{ }^\circ\text{C}$ . The

stirring speed was also set as 600 rpm to ensure no external diffusion dependence on the reaction rates. Analysis of Variance (ANOVA) was used to statistically analyse the effect of each reaction parameter on the reaction rate. The effect of catalyst type (gel-type, macroporous and hypercrosslinked poly(St-DVB) sulfonic acids) was first investigated, and the parameters of catalyst amount, temperature, molar ratio of methanol to FFAs, and particle size of catalyst were optimised over hypercrosslinked poly(St-DVB) sulfonic acid M2E catalysis. **Table 5.1** summarises the variables investigated for each parameter. In each individual experiment, one parameter was varied by fixing the other parameters to the standard conditions. The samples in the reaction mixture at each time interval were withdrawn, and the FFA content was quantified by titration with NaOH dissolved in ethanol anhydride using phenolphthalein as indicator [3, 4]. **Eq. 5.1** was used to determine the percentage conversion of FFAs at a specific time (t).

$$X_A(\text{in } \%) = \frac{100(V_0 - V_t)}{V_0}, \quad (\text{Eq. 5.1})$$

where  $X_A$  is the percentage conversion of FFAs,  $V_0$  and  $V_t$  is the volume of NaOH solution required for neutralisation at initial stage of the reaction and at the time (t).

The surface area of reused M2E was measured using a Micromeritics ASAP 2020 analyser and acid site concentration was determined by aqueous titration followed by ion exchange with NaCl solution in an Autoclave Engineers Magnedrive III instrument. The detailed procedures were the same as those in Chapter 3.

**Table 5.1.** The variables for each parameter of the reaction condition

<b>Parameter</b>	<b>Variables</b>		
<b>Catalyst type</b>	C100X4	Amberlyst 35	M2E
<b>Methanol: FFAs molar ratio</b>	8.83	12.4	17.7
<b>Catalyst amount (g)</b>	0.10	0.20	0.40
<b>Temperature (°C)</b>	50	60	65
<b>Particle size of the catalyst</b>	beads	powder	

### 5.2.3. Data handling with Analysis of Variance

Analysis of Variance (ANOVA) is a useful tool for determining the effect of each related parameter from a series of experimental data on the response performance, and it has been widely used to optimise processing conditions [5].

In the case of ANOVA that interaction of main factors affects output values, ANOVA partitions total variation into three components with the total sum of squares:

$$SS_T = SS_A + SS_B + SS_{AB}. \quad (\text{Eq. 5.2})$$

A is the factor of interest, B is the randomised block, and AB is the interaction between A and B. In the case of our investigation, A stands for the treatment of each investigated parameter and B summarises the sample analyses (known as subjects) for the variables of each parameter at different reaction time for each variable of the parameter. The sum of square for each term is:

$$SS_T = \sum_{j=1}^r \sum_{i=1}^n x_{ij}^2 - \frac{T^2}{rn}, \quad (\text{Eq. 5.3})$$

$$SS_A = \sum_{j=1}^r \frac{x_j^2}{n} - \frac{T^2}{rn}, \quad (\text{Eq. 5.4})$$

$$SS_B = \sum_{i=1}^n \frac{x_i^2}{r} - \frac{T^2}{rn}, \quad (\text{Eq. 5.5})$$

$r$  and  $n$  are the number of subjects in each group of Factor  $A$  and  $B$  respectively,  $x$  is the value of each subject and  $T$  is the sum of the total value of the subjects in ANOVA matrix [6]. The error term is caused by the  $A/B$  interaction, so it is generally given as:

$$SS_E = SS_{AB}. \quad (\text{Eq. 5.6})$$

The mean squares (MS) are calculated by dividing each sum of squares by the associated degree of freedom (df) [6]:

$$MS_A = \frac{SS_A}{(r-1)}, \quad (\text{Eq. 5.7})$$

$$MS_B = \frac{SS_B}{(n-1)}, \quad (\text{Eq. 5.8})$$

$$MS_E = \frac{SS_E}{(r-1)(n-1)}. \quad (\text{Eq. 5.9})$$

The F-value is used to test the validity of the null hypothesis. The null hypothesis states that the effect of the subject of each variable does not significantly differ in the analysed response, which is to be discounted when a statistically significant F-value is obtained [7]. F-value is the relative ratio of the variance of interest (the effect on the analysed response) to the variance of noninterest (the estimate of the error term) [6], so the relation is expressed as:

$$F = \frac{\text{Variance of Interest}}{\text{Variance of Nonintest}} = \frac{MS_A}{MS_E}. \quad (\text{Eq. 5.10})$$

The significance of the effect of the parameters on reaction activity in this esterification is reflected in the p-value which is related to the F-value. The data in our experiment were judged by 1% and 5% level of significance. For example, if  $p < 0.01$ , this means the result occurs less than once in 100 by chance, thus there is a statistically significant difference in performance on the test among the variables.

For a valid ANOVA test, several assumptions are incorporated into the formulae: the observations are independent, and are normally distributed in the population; the variance within each source is of homogeneity [7]. To note the effect on the F-value, Norton found that mild departures either from the homogeneity of variance or from normal distribution have little effect on the F distribution [8]. As a result, ANOVA is termed robust with respect to violations of assumptions underlying it as long as a design with equal numbers of subjects per level is analysed [9]. It is also to be noted that the mean square of error ( $MS_E$ ) in ANOVA is strongly affected by an outlier measurement. Therefore, to achieve relative homogeneity of the experimental data, the conversion of FFAs was replaced by percentage conversion of FFAs differentiated by reaction time ( $\Delta X_A/\Delta t$ ). The values of  $\Delta X_A/\Delta t$  are expected to be homogeneously distributed over reaction time at low conversion of FFAs where the reaction rates invariably appeared constant. Thus the data can be analysed through the ANOVA method in which each value of  $\Delta X_A/\Delta t$  is regarded as a replicate of the experiment.

Experimentally, sampling was conducted at 20 min intervals until 80 min. the experimental results for each reaction parameter are shown in **Table 5.2**.

**Table 5.2.** The experimental data ( $\Delta X_A/\Delta t$ ) used for Analysis of Variance for condition optimisation for esterification step of biodiesel synthesis

Parameters		$\Delta X_A/\Delta t$ (%/h)			
Reaction time (min)		20	40	60	80
Catalyst type	C100X4	1.88	2.81	2.50	1.41
	Amberlyst 35	18.63	16.77	14.91	13.51
	M2E	22.02	30.28	26.61	27.53
Molar ratio of methanol: FFAs	8.83	18.75	27.19	25.63	27.19
	12.4	28.57	32.65	31.97	28.06
	17.7	22.02	30.28	26.61	27.53
Catalyst amount	0.10 g	15.30	13.50	14.61	15.19
	0.20 g	22.02	30.28	26.61	27.53
	0.40 g	59.30	53.70	41.98	45.45
Temperature	50 °C	22.64	22.64	23.27	23.11
	60 °C	22.00	30.28	26.61	27.52
	65 °C	36.77	40.65	36.77	30.48
Particle size of M2E	beads	22.00	30.28	26.61	27.52
	powder	23.22	30.28	37.80	28.73

### 5.3. Results and discussion

#### 5.3.1. Catalyst activity in pure oleic acid esterification

M2D exhibits higher surface area but slightly lower acid site concentration compared to M2E (Page 48). In the pure oleic acid esterification M2D is more active than M2E in the first esterification cycle (**Fig. 5.1**). This is illustrative of the need to balance acid site concentration and surface area if optimal catalytic activity is to be achieved. When the reactant is relatively large in size, increase in surface area of the catalyst

is more advantageous than higher acid site concentration. In terms of reusability, the activity of M2E was preserved well in the second cycle, while M2D was obviously deactivated. The reason is not clear; but this might be linked to their different sulfonation routes (as has been discussed in Chapter 3). However, the objective of this chapter is to obtain the most reusable hypercrosslinked poly(St-DVB) sulfonic acid to be used as catalyst for FFA removal for biodiesel synthesis. M2E was chosen for the study of esterification of oleic acid blended with rapeseed oil.

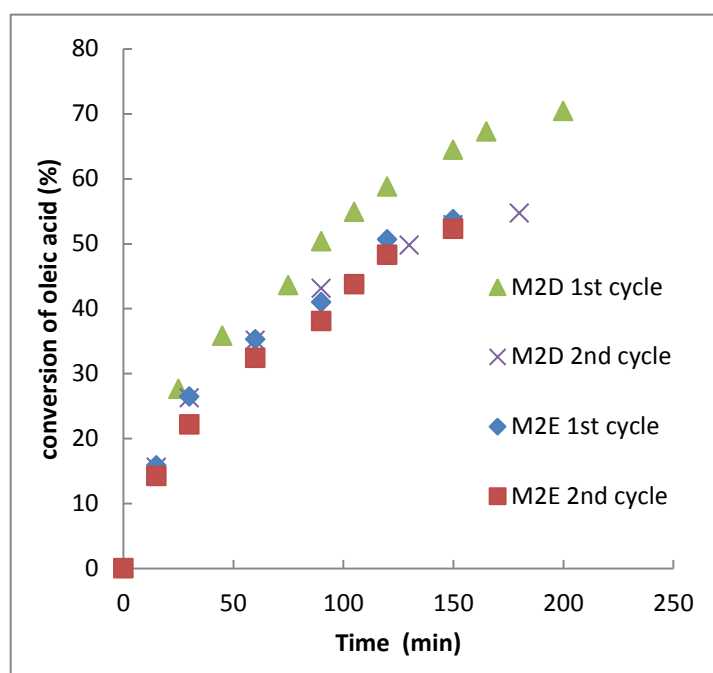


**Fig. 5.1.** Activities of M2D and M2E in pure oleic acid esterification for the first cycle and the second cycle (methanol: 20.0 g, oleic acid: 4.0 g, catalyst: 0.20 g, temperature: 60 °C, stirring speed: 600 rpm).

## 5.3.2. Catalytic performance in esterification of oleic acid blended with rapeseed oil

### 5.3.2.1. Results of Analysis of Variance

To distinguish from traditional methods for evaluating the effect of each reaction parameter on reaction kinetics, ANOVA enables the analysis from the viewpoint of statistics, which hence avoids subjective interpretation of the effect of each parameter. However, it should be noted that there are still some shortcomings of ANOVA in this optimisation analysis. Firstly, the optimisation was conducted within the variables of each parameter which were still subjectively chosen. Secondly, this work regarded the conversions ( $\Delta X_A/\Delta t$ ) at initial reaction time periods of the single reaction as the replicates. This treatment would also enlarge the error term in ANOVA, hence weakening the power of this method to reject null hypothesis.

From the ANOVA results, it is, however, still possible to say that all the parameters have a more or less positive effect on the rate of FFA conversion (**Table 5.3**). The sulfonic acid activity shows high dependence on the catalyst type, which is at the 1% significance level. The particle size of hypercrosslinked catalyst M2E has less effect on the rate of FFA conversion at the chosen judgement levels ( $p > 0.05$ ). Higher molar ratios of methanol to FFAs at the selected variables increased the reaction rate at  $p < 5\%$  level of significance. For the temperature, and catalyst concentration, there is evidence at  $p < 1\%$  level that the variations in the tested range have significantly affected reaction rate. Within the M2E catalysed esterification, the significance of the effect of each parameter on the reaction rate can be ranked as

catalyst amount > temperature > molar ratio of methanol to FFAs > catalyst size.

Based on the ANOVA results, the optimal parameters for FFA esterification in the acidic rapeseed oil are 0.40 g hypercrosslinked poly(St-DVB) sulfonic acid M2E in bead form as the catalyst, temperature of 65 °C and molar ratio of methanol to FFAs of 17.7 with stirring speed of 600 rpm, under which conditions the final FFA conversion achieved was 97.2% (**Fig. 5.2**).

**Table 5.3.** ANOVA results for the effect of each reaction condition on the reaction rate of FFA conversion in the acidic rapeseed oil

parameter	Treatment			Error			F	p
	SS	df	MS	SS	df	MS		
<b>Catalyst type</b>	1203	2	601.5	39.16	6	66.53	92.17	0.000313
<b>Molar ratio<sup>1</sup></b>	65.47	2	32.73	23.32	6	3.887	8.420	0.0181
<b>Catalyst amount</b>	2593	2	1297	172.7	6	28.79	45.03	0000244
<b>Temperature</b>	374.3	2	187.1	54.79	6	9.132	20.49	0.00209
<b>Catalyst size<sup>2</sup></b>	3.112	1	1.582	3.112	3	0.527	5.901	0.0934

1. Molar ratio of methanol to FFAs.
2. The catalyst is M2E

#### 5.3.2.2. Effect of catalyst type

For the mixture of oleic acid and rapeseed oil to react with methanol over solid acid catalysis, methanol consumption by both esterification and transesterification would be expected [10, 11]. However, under the investigated condition, less than 1% of triglycerides were transesterified. This means triglycerides are almost inert over gel-type C100X4, macroporous Amberlyst 35 and home-made hypercrosslinked M2E catalysis. In other words, the catalyst only enhanced the rate of esterification of FFAs. The interest is to compare the activity of the three generations of

styrene-based sulfonic acids in esterification of FFAs in the presence of triglycerides. The ANOVA result shows that the reaction rate strongly depends on the catalyst type. With catalyst amount, molar ratio of methanol to FFAs, temperature and stirring speed set to constant values, the superiority of hypercrosslinked M2E over Amberlyst 35 and C100X4 can be seen in **Fig. 5.2**. Generally, the relative activity order of the catalysts followed their order of degree of cross-linking (C100X4 < Amberlyst 35 < M2E) which is also reflected by their relative BET surface areas. The extremely low p-value was due to the poorest activity of C100X4. Less than 5 % of FFAs was converted on C100X4 in 1500 minutes. It is generally known that the gel resins with light crosslinking only have high swelling capacity in the presence of polar media [12]. Good performance of gel-type catalyst was observed in the presence of more hydrophilic reaction mixtures such as liquid phase ethyl *tert*-butyl ether synthesis [13] and transesterification of isopropyl acetate with ethanol [1]. However, in the more hydrophobic mixture where a large amount of triglycerides is present, high activity in FFA esterification would only be performed by more hydrophobic resin [14]. As a consequence, M2E yielded the highest amount of methyl ester from FFAs during the same time of reaction. With the highest activity, M2E was used as the catalyst to test the effect of reaction parameters on the rate of esterification of acidic rapeseed oil.

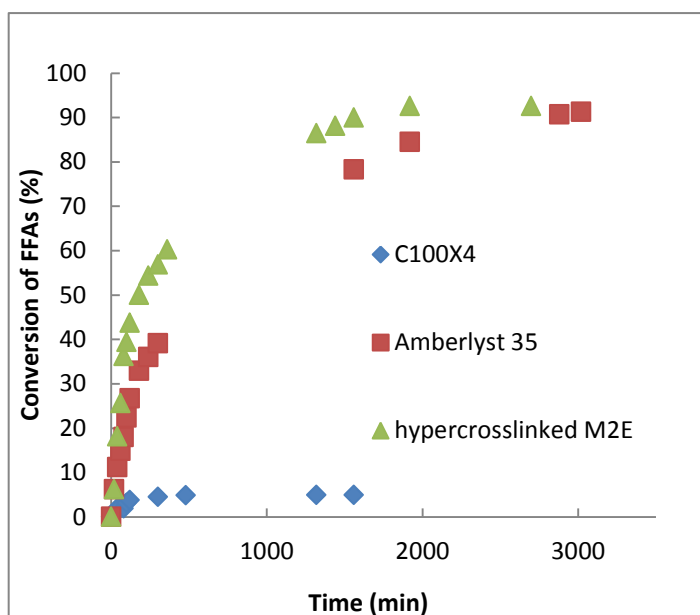


**Fig. 5.2.** Effect of catalyst type on the conversion of FFAs in the rapeseed oil (catalyst in beads: 0.20 g, methanol: 5.00 g, acidic oil: 16.0 g, temperature: 60 °C, stirring speed: 600 rpm).

### 5.3.2.3. Effect of molar ratio of methanol to FFAs

The esterification reactions were performed in excess methanol in order to favour the forward reaction. The effect of molar ratio of methanol to FFAs was studied at the ratios of 8.83:1, 12.4:1 and 17.7:1 over M2E catalysis (**Fig 5.3**). The ratio was adjusted by increasing the amount of methanol while keeping the quantity of acidic oil constant. Minor transesterification under this condition was detected, so the effect of molar ratio of methanol to FFAs on the FFA conversion was only due to the esterification. It was expected that a higher molar ratio of methanol to FFAs would increase the rate of reaction as well as the equilibrium conversion of FFAs. This agreed with the experimental results, as the equilibrium conversion shifted from 92.6% to 97.2% and the reaction proceeded faster with the increase of molar ratio of methanol to FFAs from 12.4 to 17.7. However, ANOVA analysis revealed that at

the initial stage of the reaction the molar ratio of methanol to FFAs is a less significant parameter that affects the reaction rate ( $p>0.01$ ). This is because the increase in the quantity of methanol led to the decrease of catalyst concentration in the reaction mixture, subsequently lowering the chance of effective collision between the FFAs and the catalyst. Strictly speaking, evaluation of the effect of molar ratio is not easily practical, because varying the reactant molar ratio always companies varied catalyst concentration or change in the total volume of the reaction mixture, both of which would affect the reaction rate. The method for evaluating the effect of reactant molar ratio on the reaction kinetics is not always addressed by the researchers in the papers.

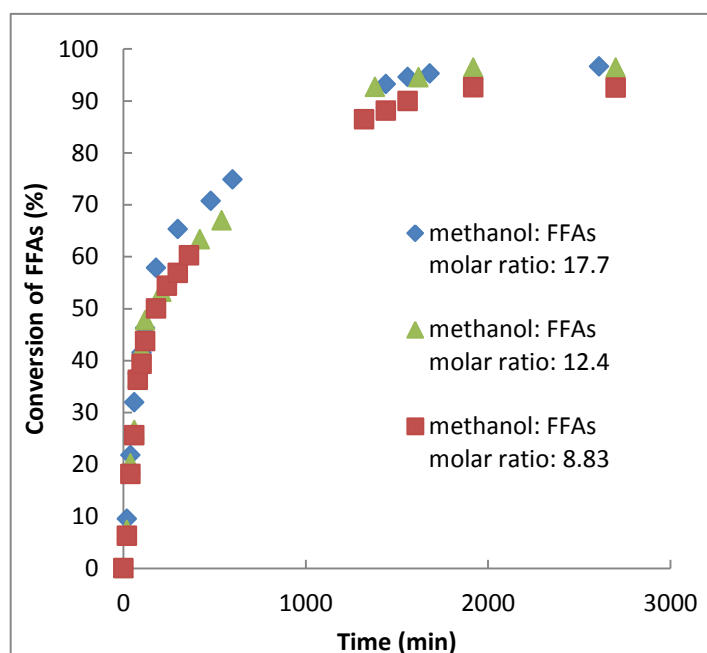


**Fig. 5.3.** Effect of molar ratio of methanol to FFAs on the conversion of FFAs in rapeseed oil over hypercrosslinked poly(St-DVB) sulfonic acid M2E catalysis (catalyst in beads: 0.20 g, temperature: 60 °C, stirring speed: 600 rpm).

#### 5.3.2.4. Effect of catalyst amount

In general, a higher catalyst amount would increase the frequency of collision, hence increasing the reaction rate. This effect was observed when the M2E amount was varied from 0.10 g to 0.40 g (**Fig. 5.4**). As the catalyst amount increased, the trend of difference in the FFA conversion became smaller. This indicates that the benefits of increasing catalyst amount reduced when the number of active acid sites was close to being sufficient for conversion of the reactants. This trend also predicts that there would be a maximum catalyst amount that enhances the reaction rate, and that beyond that amount adding more catalyst is not effective in experiments [15]. Additionally, some researchers claimed increasing catalyst amount also enhanced the final conversion of the acid in esterification [16, 17]. This was not observed in FFA esterification catalysed by M2E, and it is believed that the equilibrium conversion of FFAs should be independent of catalyst amount, which follows the Le Chatelier's principle.

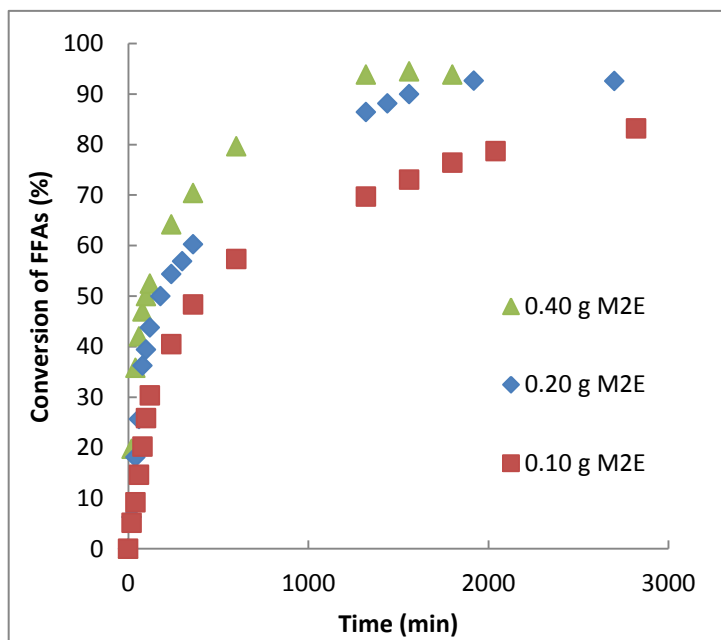


**Fig. 5.4.** Effect of catalyst amount on the conversion of FFAs in rapeseed oil over hypercrosslinked poly(St-DVB) sulfonic acid M2E (beads) catalysis (methanol: 5.00 g, acidic oil: 16.0 g, temperature: 60 °C, stirring speed: 600 rpm).

#### 5.3.2.5. Effect of temperature

As an endothermic reaction, the esterification of FFAs is favoured by higher temperature. It is shown in **Fig. 5.5** that the final FFA conversion differed from 89.6% to 93.5% when temperature was increased from 50 °C to 65 °C. Higher temperature accelerates the forward reaction, so the experiment at 65 °C reached the equilibrium position faster than the other two. However it is necessary in that, temperatures higher than 65 °C with the batch-wise setup are not practical for the esterification reaction with methanol because they are beyond the boiling point of methanol.

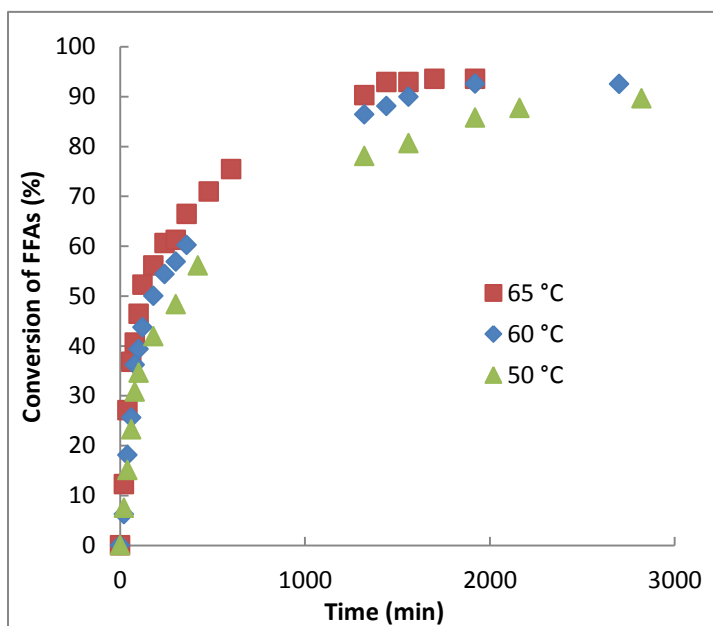


**Fig. 5.5.** Effect of temperature on the conversion of FFAs in rapeseed oil over hypercrosslinked poly(St-DVB) sulfonic acid M2E catalysis (catalyst in beads: 0.20 g, methanol: 5.00 g, acidic oil: 16.0 g, stirring speed: 600 rpm).

#### 5.3.2.6. Effect of particle size of the catalyst

There are two types of mass transfer resistance in heterogeneous catalysis. External mass transfer resistance has been eliminated with the stirring speed of 600 rpm. Internal mass transfer was assessed because acid site accessibility directly relies on internal mass transfer. The comparison was made between the activities of the beads and powder forms of M2E. The effect of particle size of catalyst was tested with ANOVA analysis and it showed no difference in catalytic performance of M2E at 5% significance level for the two forms. This finding suggests that no internal mass transfer resistance occurred using the M2E beads for esterification of FFAs. Though catalysis is dominated by acid sites that are close to the catalyst surface, the internal acid sites of the hypercrosslinked catalyst are also readily accessible to FFAs.

To facilitate the recycling process, it is better to use the catalyst in the form of beads.

**Table 5.4.** Summary of the BET surface area and acid site concentration of M2E before the first cycle and after the second cycle of esterification of oleic acid blended with rapeseed oil

	BET surface area (m <sup>2</sup> /g)	Acid site conc. (mmol/g) <sup>1</sup>
<b>Before first cycle</b>	458	0.78
<b>After second cycle</b>	327	0.59

1. Error:  $\pm$  0.03 mmol/g.

#### 5.3.2.7. Catalyst reusability and deactivation

Catalyst reusability of the hypercrosslinked poly(ST-DVB) sulfonic acid M2E in esterification of oleic acid blended with rapeseed oil was evaluated by performing consecutive batch runs on the standard reaction conditions as stated in the experimental design section. It can be seen from **Fig. 5.6** that the activity M2E decreased on going to the second cycle. The surface area of reused M2E decreased from 458.4 m<sup>2</sup>/g to 327.1 m<sup>2</sup>/g (**Table 5.4**) after the second cycle of the reaction. This could be attributed to blockage of the fine pores by large molecules such as triglycerides. Moreover, the acid site concentration was observed to decrease from 0.78 mmol/g to 0.59 mmol/g after the second reaction cycle. Considering there would be some FFA molecules trapped in the catalyst pores, the true acid site concentration of M2E after the second cycle would be lower than 0.59 mmol/g. Russbueltdt and Hoelderich explained the acid site loss of the polymer supported sulfonic acid in esterification of FFAs would be caused by continuous neutralisation

of sulfonic acid groups with salt contaminants presented in the oil feedstock [2]. This might also have occurred in our investigated case. Additionally, leaching of sulfonic acid groups could also be responsible for the decreased activity of M2E, considering the long-time interaction (over 2500 minutes) of M2E with the reactants in each reaction cycle.

It is also noted that sulfonic acid on hypercrosslinked poly(St-DVB) is more vulnerable to leach out when contacted with polar liquids (Chapter 2). This might suggest methanol used in excess would not be suitable for the FFA esterification over hypercrosslinked poly(St-DVB) sulfonic acid catalysis because methanol potentially accelerates the rate of acid site leaching. It has been reported that to FFA conversion within 10 % decrease over D5081 was sustained for 6 cycles applying 1:1 stoichiometric alcohol-to-acid molar ratio in the Carberry reactor, with each cycle lasting for 6 hours [18]. Andrijanto et al reported the activity of D5081 was retained in oleic acid esterification on repeated use with pressurised reactor at temperature of 85 °C. They suggested organic deposition on the catalyst surface would be prevented by fast diffusion of FFAs [14]. From this point of view, hypercrosslinked poly(St-DVB) sulfonic acid would be more reusable for the FFA esterification if a lower amount of methanol is used with a suitable reactor configuration. A continuous flow reactor may be advantageous. It could not only enhance reusability of the hypercrosslinked poly(St-DVB) sulfonic acid by reducing the amount of methanol, but also enhance the activity by increasing the reaction temperature and the products would be continuously removed.

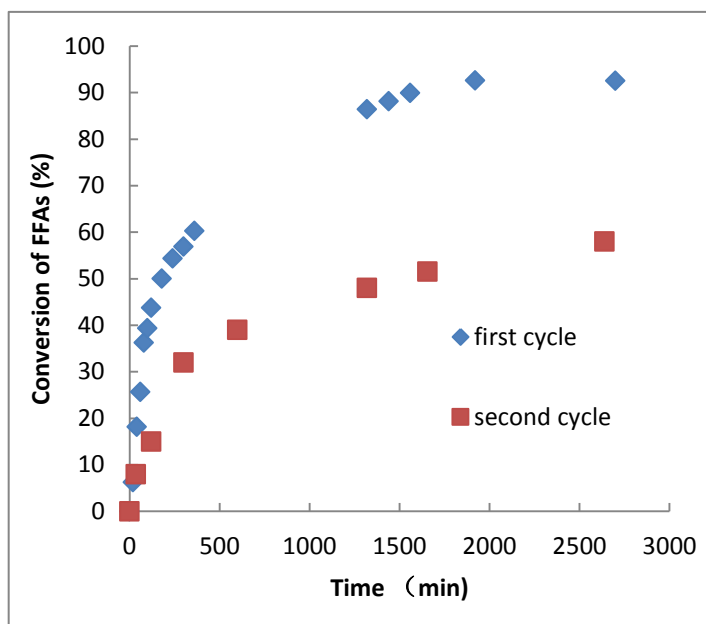


**Fig. 5.6.** Reusability study of M2E catalyst on esterification of oleic oil with methanol in the presence of rapeseed oil (catalyst in beads: 0.20 g, methanol: 5.00 g, acidic oil: 16.0 g, temperature: 60 °C, stirring speed: 600 rpm).

#### 5.4. Summary of results

M2D is more active but less reusable in the esterification of pure oleic acid than M2E. M2E is more active than macroporous Amberlyst 35 and gel-type C100X4 in the esterification of oleic acid blended with rapeseed oil. The effect of each reaction parameter on the rate of esterification of acidic oil over M2E catalysis was analysed with ANOVA. Increase in catalyst amount was found to be the most significantly effective, followed by increasing temperature, molar ratio of methanol to FFAs and decreasing the catalyst particle size. Reusability study of M2E reveals deactivation occurred in the successive cycle. The reason was speculated to be pore blockage and acid site loss of the catalyst. Suggestion for avoiding the deactivation was to use more suitable reactor configurations.

## References

- [1] C. N. Rhodes, D. R. Brown. S. Plant and J. A. dale, *React. & Funct. Polym.*, 40 (1999) 187-193.
- [2] B. M. E. Russbuedt and W. F. Hoelderich, *Appl. Catal. A: Gen.*, 362 (2009) 47-57.
- [3] J. Kucharsky and L. Safarik, *Titrations in Non-aqueous Solvents*, Elsevier, London, 1965.
- [4] N. Ozbay, N. Oktar and N. A. Tapan, *Fuel* 87 (2008) 1789-1798.
- [5] B. M. Gopalsamy, B. Mondal and S. Ghosh, *J. Sci. & Ind. Res.*, 68 (2009) 686-695.
- [6] W. C. Guenther, *Analysis of Variance*, Prentice-Hall, Englewood Cliffs, 1964.
- [7] J. R. Turner and J. F. Thayer, *Introduction to Analysis of Variance*, Sage Publications, Thousand Oaks, 2001.
- [8] H. R. Barker and B. M. Barker, *Multivariate Analysis of Variance*, the University of Alabama Press, Alabama, 1984.
- [9] M. J. Roberts and R. Russo, *A Student's Guide to Analysis of Variance*, Routledge, London, 1999.
- [10] K. Suwannakarn, E. Letero, K. Ngaosuwan and J. G. Goodwin, Jr., *Ind. Eng. Chem. Res.*, 48 (2009) 2810-2818.
- [11] A. Alsalmeh, E. F. Kozhevnikova and I. V. Kozhevnikov, *Appl. Catal. A: Gen.*, 349 (2008) 170-176.
- [12] M. L. Honkela, A. Root, M. Lindblad and A. O. I. Krause, *Appl. Catal. A: Gen.*, 295 (2005) 216-223.
- [13] M. Umar and D. Patel and B. Saha, *Chem. Eng. Sci.*, 64 (2009) 4424-4432.
- [14] E. Andrijanto, E. A. Dawson and D. R. Brown, *Appl. Catal. B: Envir.*, 115-116 (2012) 261-268.
- [15] M. Kolyaei, G. Zahedi and M. M. Nasef, 4<sup>th</sup> International Conference of Modelling, Simulation and Applied Optimization, Kuala Lumpur (2011) 1-5.
- [16] S. Gan, H. K. Ng, P. H. Chan and F. L. Leong, *Fuel Proc. Technol.*, 102 (2012) 67-72.
- [17] C. S. Caetero, L. Guerreiro, I. M. Fonseca, A. M. Ramos, J. Vital and J. E. Castanheiro, *Appl. Catal. A: Gen.*, 359 (2009) 41-46.
- [18] D. C. Boffito, C. Pirola. F. Galli, A. Di Michele and C. L. Bianchi, *Fuel*, 108 (2013) 612-619.

## Chapter 6

### Conclusion and Suggestions for Future Work

#### 6.1. Conclusion

##### 6.1.1. Hypercrosslinked poly(St-DVB) sulfonic acids: activity and reusability

Purolite D5081, D5082 and the home-made hypercrosslinked poly(St-DVB) sulfonic acids showed high activities in esterification of carboxylic acids with methanol. The hypercrosslinked polymers differ from the macroporous ones in that they possess a second cross-linking by methylene bridges. The acid site concentrations of the home-made catalysts range from 0.42 mmol/g to 0.78 mmol/g, with corresponding surface area varied from 657.2 m<sup>2</sup>/g to 458.4 m<sup>2</sup>/g. Though exhibiting lower acid concentration than macroporous catalysts, the hypercrosslinked catalysts have more effectively accessible acid sites to the reactants with a wide range of molecular size, so they showed higher activities than Amberlyst 35 in esterification of oleic acid with methanol. The relative activities of hypercrosslinked catalysts are strongly in line with the corresponding acid site concentrations.

Reusability of the hypercrosslinked poly(St-DVB) sulfonic acids is a great concern throughout the project. First of all, the link between catalyst deactivation in consecutive reaction cycles of esterification of acetic acid with methanol and the loss of acid sites of D5081 and D5082 was established. This suggests acid sites in hypercrosslinked polymer networks would leach out in contact with the reactants.

Further investigation revealed that the leaching is highly related to the polarity of contacting liquid, i.e. acid sites leach out in polar liquids. In water, two thirds of the acid sites leach out from D5081. By studying the temperature dependence on the leaching rate, it was found that the leaching species is mainly sulfuric acid trapped in the polymer. Therefore, the home-made hypercrosslinked poly(St-DVB) sulfonic acids were thoroughly washed to remove the trapped acid species, before they were used in the esterification of acetic acid and oleic acid with methanol. However, catalyst deactivation still occurred in the oleic acid esterification in the presence of rapeseed oil stimulating FFAs removal for biodiesel synthesis. It was speculated that this would be due to pore blockage by large molecules such as triglycerides in addition of acid site leaching or cation exchange with metal ions in the oil. The use of a suitable reactor configuration was suggested to prevent the deactivation of hypercrosslinked poly(St-DVB) sulfonic acids for FFA esterification.

#### 6.1.2. Statistical study: kinetic modelling and optimisation of reaction conditions

This work presents the first kinetic modelling of acetic acid esterification catalysed by hypercrosslinked poly(St-DVB) sulfonic acid M2E in which acid site leaching is absent in short-time contact with the reactants. The analysis was conducted by fitting initial reaction rates to various kinetic models. The Eley-Rideal model (**Eq. 6.1**) was found to best fit the experimental data. This derived model enables to predict the reaction profiles over hypercrosslinked poly(St-DVB) sulfonic acid M2E

with various molar ratios of methanol to acetic acid at catalyst amount of 0.200 g and 60 °C. The kinetic expression for the acetic acid esterification is

$$\frac{dX_A}{dt} = \frac{0.00269C_{A,0}}{1 + C_{A,0}[0.0536(n - X_A) + 0.0267(1 - X_A) + 5.49X_A]} \times \left[ (n - X_A)(1 - X_A) - \frac{X_A^2}{10.9} \right], \quad (\text{Eq. 6. 1})$$

Where  $X_A$  is the conversion ratio of acetic acid,  $t$  is reaction time,  $C_{A,0}$  is the initial concentration of acetic acid,  $n$  is the initial molar ratio of methanol to acetic acid.

In the esterification of oleic acid blended with rapeseed oil, the reaction conditions were optimised to be 0.40 g hypercrosslinked catalyst M2E in bead form, methanol-to-FFA molar ratio of 17.7, and temperature of 65 °C and stirring speed of 600 rpm to achieve the final FFA conversion of 97.2%. Analysis of Variance (ANOVA) was introduced to evaluate the effect of each reaction condition on the reaction rate. For the three generation of styrene-based sulfonic acids, the activity order was ranked as hypercrosslinked M2E > macroporous Amberlyst 35 > gel-type C100X4. The rate dependence on the change of each reaction condition was ordered as catalyst amount > temperature > molar ratio of methanol to FFAs > catalyst size.

## 6.2. Suggestions for future work

### 6.2.1. More characterisation techniques

Sulfur content analysis should be conducted to ascertain the accuracy of titration method for determination of the acid site concentration of the catalysts, provided

that one sulfur atom is associated with one acidic proton in the thoroughly washed resin. Higher sulfur content detected in the hypercrosslinked polymer supported sulfonic acids can help the determination of trapped amount of sulfuric acid in the fresh resins. Relative acid site accessibility, which is influential upon the catalyst activity, can be characterised using base adsorption calorimetry [1]. Additionally, the relationship between acid site strength and the activity of the hypercrosslinked polymer supported sulfonic acids in esterification reactions is to be established using base adsorption calorimetry [2].

#### 6.2.2. Improvement of the kinetic model

Though the proposed Eley-Rideal model is able to predict the kinetic profiles of the esterification reaction, the effect of reaction temperature and catalyst amount should also be included in the kinetic expression. The temperature (T) dependence of the reaction rate can be expressed with the Arrhenius equation:

$$\ln k = -\frac{E_a}{R} \left( \frac{1}{T} \right) + \ln A. \quad (\text{Eq. 6.2})$$

where k is the rate constant, T is the temperature,  $E_a$  is the activation energy, R is the universal gas constant and A is the exponential factor. A fixed amount of catalyst is usually applied for kinetic modelling of a catalysed reaction. The catalyst amount is noted to be proportional to the reaction rate in well-established kinetic models. However, this is not always true because there would be an optimum point beyond which the catalyst sites will be in excess and the reaction rate thereafter remains constant. Therefore, in a specific kinetic model, the optimal range for the

catalyst should be captioned. This can be done by depicting the effect of varied amounts of the catalyst on the reaction rate.

### 6.2.3. Suitable reactor configuration

All the experiments in this project were conducted in the batch reactor where continuously produced water kept inhibiting activity of the catalysts. It is worth investigating the application of different reactor configurations that would effectively remove water to enhance the catalyst activity and reusability. Continuous flow systems, such as spray tower loop reactors and fixed-bed reactors [3, 4], should be evaluated and might be advantageous for the use of hypercrosslinked poly(St-DVB) sulfonic acid catalysts for esterification of carboxylic acids with methanol. Firstly, the temperature can be raised over boiling point of methanol to increase the reaction rate [5]. Secondly, the higher temperature could possibly drive the organic deposition to diffuse out of the catalyst surface. Thirdly, higher product yields are to be obtained because the equilibrium will shift toward the product, which results from continuous removal of water [3]. Fourthly, with continuous water removal, the catalyst is prevented from poisoning by water. Fifthly, methanol used in excess is not required, which also avoids long-time methanol/catalyst interaction hence reducing the possibility of acid site leaching from the catalyst.

## References

- [1] S. P. Felix, C. Savill-Jowitt and D. R. Brown, *Thermochimica Acta* 433 (2005) 59-65.
- [2] P. F. Siril, H. E. Cross and D. R. Brown, *J. Mol. Catal. A: Chem.*, 279 (2008) 63-68.
- [3] S. M. Son, H. Kimura and K. Kusakabe, *Bioresour. Technol.*, 102 (2011) 2130-2132.
- [4] E. Santacesaria, R. Tesser, M. Di Serio, M. Guida, D. Gaetano, A. Garcia Agreda and F. Cammarota, *Ind. Eng. Chem. Res.*, 46 (2007) 8355-8362.
- [5] S. Shanmugam, B. Viswanathan and T. K. Varadarajan, *J. Mol. Catal. A: Chem.*, 223 (2004) 143-147.